UNIVERSITÁ DEGLI STUDI DI BERGAMO
SCHOOL OF ENGINEERING
DEPARTMENT OF ENGINEERING AND APPLIED SCIENCES
DOCTORAL PROGRAMME IN ENGINEERING AND APPLIED SCIENCES

VISIBLE LIGHT PHOTOCATALYST FOR WATER PURIFICATION AND SELF-CLEANING COATINGS

Doctoral Thesis of

Elena Luisa de la Fuente García

Supervisor:

Chiar.ma Prof.ssa Isabella Natali Sora

Tutor:

Chiar.ma Prof.ssa Francesca Fontana

The Chair of the Doctoral Program:

Chiar.mo Prof. Valerio Re

A.Y. 2017/2018 – XXX Cycle

Science never solves a problem without creating ten more

George Bernard Shaw

A Daniele y Pablo

Abstract

Pollution in water and atmosphere is a growing concern in the current society and demands short-term solutions. Conventional purification techniques like biological treatment, direct oxidation, etc. cannot eliminate low concentrations or some of the so-called emerging pollutants (hormones, detergents, pharmaceuticals, etc.) thus calling for the use of advanced oxidation processes (AOP), namely, techniques in which highly oxidising agents (mostly OH radicals) are produced to degrade organics compound, bacteria and viruses, reaching the complete mineralization or, at least, producing nontoxic by-products. One of these techniques is heterogeneous

photocatalysis: redox reactions are developed on the surface of a solid catalyst that is activated by light. Nowadays the more employed and studied photocatalyst is titanium dioxide (TiO_2). Its commercial applications are very diverse, including self-cleaning materials (cements, paints), antifogging materials (mirrors, glasses) and water and air purification devices. The operating limits of this effective photocatalyst are in the fact that it needs UV radiation to be activated, due to its relatively wide band gap (3.2 eV). This is a significant problem in economic terms, for high energy costs, in healthy terms, since UV radiation is dangerous for sight and skin, and it is a limit to the use of sunlight, as only 4 % of the solar spectrum that reaches the Earth surface is in the UV range. To overcome this problem, investigations are focused on TiO_2 modifications to render it active with visible light (doping with metal and non-metal ions, coupling with other semiconductors, etc) as well as on the use of other semiconductors with narrower band gap.

A ceramic material, lanthanum orthoferrite ($LaFeO_3$), with ionic and electronic semiconductor properties, is synthesized in our laboratory since 2008 [1] and it is studied for its application in the combustion cells [2]. Knowing that it also works as photoconductor under visible light [3], it can be considered a good candidate to be used as visible light photocatalyst. Its effectiveness in the degradation of organic dyes and other molecules has been reported [4].

After the successful degradation of organic compounds in the slurry tests carried up with the $LaFeO_3$ powders, our group started to develop deposition systems in order to avoid filtration problems, such

as loss of catalyst and costs, thus rendering the reuse of the photocatalyst easier to achieve a practical applicability. In the present thesis two deposition methods were studied: the preparation of a photocatalytic paint and the deposition of the catalyst over a ceramic foam by dip-coating process.

In the first part of the work, $LaFeO_3$ was added to a commercial water based paint. This innovative photocatalytic paint has been tested to prove two aspects:

- Its self-cleaning performances, following the degradation of an azo dye under visible light irradiation.
- The paint durability, executing accelerated ageing tests in a climatic chamber, and subsequently verifying visible alterations and possible diminution of its self-cleaning performances.

In the second part, the objective was the application of the material for the wastewater treatment. In collaboration with the Universidad de Las Palmas de Gran Canaria a handy and resistant photocatalytic foam was developed, to avoid the vigorous continuous stirring required to keep powder in slurry and the necessary filtration after the reactions to reuse the photocatalyst. The support chosen was a commercial ceramic inert porous material (foam) and the deposition method was the dip-coating technique.

To apply this coating technique high quantities of catalyst had to be used because it required the preparation of a very concentrate solution. For this reason and for a possible scaling up, the production

rate of the photocatalyst in our laboratory had to be increased. The quality of the catalyst had been largely tested for low production rates. Theoretically the results of the synthesis must be the same; however, a complete characterization and determination of photocatalytic performances were carried out on three batches of catalyst prepared on a large scale.

The photocatalytic foam and the different batches in slurry were tested in the degradation of 4-Nitrophenol. A comparison between the slurry test and the fixed bed test is presented.

KEY WORDS

$LaFeO_3$, self-cleaning, wastewater, photocatalysis, paint, dip-coating, 4-nitrophenol, photocatalytic foam.

Summary

A cheap and effective photocatalyst synthesized in our laboratory at the University of Bergamo, proved to be sensitive in the visible range of the solar spectrum. To achieve commercial application of this material, presently available in the form of nanopowder, it should be made easier to handle. Therefore, aim of this thesis is to study two different deposition techniques: mixing of the powder into a paint to create a photocatalytic coating and supporting of the powder onto a ceramic foam. The work is divided into seven chapters:

_Chapter 1: General Introduction: State of art. In this chapter, the application of Advanced Oxidation Processes (AOPs) to the

oxidation of refractory organic pollutants will be presented and among AOPs Heterogeneous Photocatalysis will be analysed; different photocatalysts will be shown and interest will be focused on lanthanum ferrite ($LaFeO_3$).

_Chapter 2: Aims of the thesis. The two objectives of the present work will be explained: the photocatalytic paint studies and the deposition on a ceramic foam of lanthanum ferrite by dip-coating.

_Chapter 3: Materials and methods. Main chemicals, materials, characterization and analytical techniques employed in this project will be shown in this section.

_Chapter 4: Characterization of the photocatalyst ($LaFeO_3$). Forbidden energy band gap, FTIR, SEM, DRX and TGA analysis are reported here.

_Chapter 5: Self-cleaning paint. The preparation of the paint, the durability studies, the air purification test and the self-cleaning tests will be detailed here.

_Chapter 6: Catalyst deposition on alumina foam. The deposition system, the degradative effectiveness compared to the catalyst in slurry as such as well as the reuse possibility will be analysed in this chapter.

_Chapter 7: Conclusions and future perspectives. Main results and further tests or modifications, interesting for the development of the materials that have surged from this study, will be foreseen.

CONTENTS

LIST OF FIGURES

BSE
BackScattered Electron images, 83, 88

DRS
Diffuse Reflectance Spectrometry, 41, 43, 54, 79, 116

FTIR
Fourier Trransform InfraRed Spectroscopy, 53, 62, 63, 66, 67, 69, 84, 85, 116

HPLC
High-Performance Liquid Chromatograph, 44, 55, 56, 100, 103

LF
Photocatalytic paint, 72, 73, 75, 78, 79, 80, 81, 83, 84, 85, 86, 87

LFW
Weathered photocatalytic paint, 79, 80, 81, 83, 84, 85

P
Reference paint, 73, 75, 79, 80, 84, 87

PW
Weathered reference paint, 79, 80, 81, 83, 84

SEM
Scanning Electron Microscopy, 52, 83, 84

TGA
Thermogravimetric analysis, 53, 62, 116

CHAPTER 1 GENERAL INTRODUCTION: STATE OF ART

1.1 Advanced Oxidation Processes (AOP's)

The World Water Vision that was presented by the World Commission on Water for the 21st Century at the Second World Water Forum in March 2000 in The Hague, the Netherlands is:

"A world in which all people have access to safe and sufficient water resources to meet their needs, including food, in ways that maintain the integrity of freshwater ecosystems. The Vision exercise's ultimate purpose is to generate global awareness of the water crisis that women and men face and of the possible solutions for addressing it. This awareness will lead to the development of new policies and legislative and institutional frameworks. The world's freshwater resources will be managed in an integrated manner at all levels, from the individual to the international, to serve the interests of humankind and planet Earth-effectively, efficiently, and equitably".

The water is a necessary and indispensable good and our lifestyle heavily impact on water supplies. Industrial, agriculture and urban wastewater, either pre-treated or untreated, end into rivers, seas and lakes, rendering the access to clean and safe water sources difficult or impossible for an important percentage of humans and animals on

Earth. This situation has led for the last 30 years to the development of filtration and purification water plants. However, traditional treatments like biological treatment, direct oxidation, inverse osmosis, etc. cannot eliminate low concentrations or some of the so-called emerging pollutants (hormones, detergents, pharmaceuticals, etc.) thus calling for the use of Advanced Oxidation Processes (AOP's), namely, techniques in which highly oxidising agents (mostly OH radicals) are produced to degrade organic compounds, bacteria and viruses, reaching their complete mineralization or, at least, transforming them into nontoxic by-products.

AOPs can be divided, based on the mechanism of radical generation, in photochemical and non-photochemical processes (Table 1.1).

Table 1.1 Classification

NON-PHOTOCHEMICAL METHODS	**PHOTOCHEMICAL METHODS**
_Ozonation in alkaline media (O_3, OH^-) _Ozonation with hydrogen peroxide (O_3/ H_2O_2, O_3/ H_2O_2/OH^-) _Fenton processes (Fe^{2+}/H_2O_2) _Electrochemical oxidation _Advanced oxidation with ultrasounds. (O_3 US, H_2O_2 US) _Radiolysis by fast neutron and fast electrons _Non-thermal plasma _Electrohydraulic charge and Ultrasonic	_Oxidation in sub and super critical water _Water photolysis with vacuum Ultraviolet (UVV) _UV/H_2O_2, UV/O_3 and UV/H_2O_2/O_3 _Photo-Fenton systems (Fe^{3+}/H_2O_2/UV) _ Heterogeneous photocatalysis

The AOP's advantages versus other techniques are:

- Destructive methods, chemically transforming the pollutants.
- Can achieve complete mineralization.
- They usually do not lead to sludge formation.
- Very useful for refractory pollutants elimination.
- Degrade low concentration of contaminants (ppb)
- Less by-products are formed.
- Effective in lowering the concentration of compounds formed by conventional pretreatments.
- Generally, improve the water organoleptic conditions.
- Useful as pretreatment for refractory pollutants, leading to the formation of biologically treatable compounds by cheaper methods.

Some of the most used AOPs methods are briefly analysed bellow indicating its advantages and disadvantages:

_Ozonation in alkaline media (O_3, OH^-)

Advantages:

Good know-how on gas-liquid reactor technologies.

Flexibility to treat different concentrations and flow rates.

Easy automatization.

Disadvantages:

Low O_3 solubility in water.

Possible formation of bromates.

O_3 production costs.

Carbonates, bicarbonates and other radical acceptors are usually present.

_Ozonation with hydrogen peroxide (O_3/ H_2O_2 and O_3/ H_2O_2/OH^-)

Advantages:

Efficiency and high degradation rate.

Capability for the degradation of basically any compound.

High how-know technology and easy automatization.

Disadvantages:

Low O_3 solubility in water.

Bromates possible formation.

O_3 and H_2O_2 production costs.

Carbonates, bicarbonates and other radical acceptors are usually present.

_Advanced oxidation with ultrasounds. (O_3 US, H_2O_2 US)

Advantages:

Less chemicals required; therefore, reduction costs.

Combination with other oxidation processes is possible.

Disadvantages:

Intensive energetic process.

_Fenton processes (Fe^{2+}/ H_2O_2)

Advantages:

Tested and industrially applicated.

Effective as pretreatment.

Disadvantages:

Homogeneous catalyst is employed.

Iron hydroxide sludges are generated.

Careful pH control is required.

Organic acids may trap iron ions.

_Photo-Fenton processes (Fe^{3+}/ H_2O_2/UV)

Advantages:

Less sludges generation respect to traditional Fenton method.

High reaction rate and possible reduction of reactor size.

Disadvantages:

Homogeneous catalyst is employed.

Low radiation efficiency.

Careful pH control is required.

Organic acids may trap iron ions.

_UV/H_2O_2, UV/O_3 and UV/H_2O_2/O_3

Advantages:

Very high oxidation rate.

Less chemicals quantity necessary; therefore, reduction costs.

Disadvantages:

Hight UV radiation generation costs.

Low radiation efficiency.

For the process viability, the pollutant must absorb in the UV range.

_Heterogeneous photocatalysis

Advantages:

Solar energy can be used directly, ecofriendly energy source.

Catalyst reuse is possible.

Combination with other oxidation methods is feasible.

Disadvantages:

Reduced efficiency without the use of oxidants substances.

Low radiation efficiency.

For the process viability, the pollutant must absorb in the UV range.

1.2 Heterogeneous photocatalysis

Heterogeneous photocatalysis consists of the photo-excitation of a solid semiconductor by the absorption of electromagnetic radiation.

Some semiconductor materials may be excited by photons with sufficient energies, creating electrons-hole pairs when an electron is promoted to the conduction band and consequently a hole is generated in the valence band. These charge carriers are able to induce reduction or oxidation respectively. The reactions that take place on the surface of the photocatalyst are well understood and can be illustrated as follows [5]:

1. Absorption of efficient photons, hν ≥ EG, by the catalyst

$$Catalyst + h\nu \Rightarrow e_{CB}^{-} + h_{VB}^{+}$$

2. Oxygen adsorbed reduction

$$O_{2\ ads} + e_{VB}^{-} \Rightarrow O_2^{\cdot -}$$

3. Neutralization of OH- groups by holes producing OH· radicals.

$$\left(H_2O \Leftrightarrow H^+ + OH^-\right)_{ads} + h_{VB}^{+} \Rightarrow H^+ + OH^{\cdot}$$

4. Oxidation of the adsorbed reactants via successive attacks by hydroxyl radicals

$$R + OH^{\cdot} \Rightarrow R^{\cdot} + H_2O$$

5. Direct oxidation by reaction with holes

$$R + h_{VB}^{+} \Rightarrow R^{\cdot +} \Rightarrow degradation\ products$$

Holes have an extremely positive oxidation potential and should thus be able to oxidize almost all chemicals. The organic radicals ($R^{\cdot}$) may react directly with O_2 and subsequently degrade to CO_2 and H_2O.

Numerous observations can indeed be explained by the intermediacy of OH·. However, due to the short life-time and high reactivity of this radical no experimental evidence for the formation of hydroxyl radicals has been given so far. It is a frequent practice to bubble air during the reaction but authors [6], [7] report that the performance does not depend on aeration. The absorption of oxygen by the surface of solution is sufficient for photocatalytic oxidation

(PCO). This means that the absorption of oxygen by the liquid phase is not the stage limiting the process rate.

Different semiconductors can be used in heterogeneous photocatalysis processes (ZnO, ZnS) but the most applied and hence more studied is titanium dioxide (TiO_2). Four are the polymorphic structures in which it can be found in nature: rutile, anatase, brookite and akaogiite (high pressure form). The first one is usually employed as white pigment and solar screen in common commercial products such as sunscreens, paints, toothpastes, etc. The second one is the photocatalytic form. The abundance of the third and the fourth ones is much lower compared with anatase and rutile forms. Several studies show that the combination of anatase and rutile is the most effective photocatalytic system.

The energy bandgap of anatase (3.2 eV) allows its activation by UV illumination with a wavelength up to 387.5 nm. At the ground level, solar irradiation starts at a wavelength of about 300 nm.

Almost all kinds of toxic chemicals are degradable by photocatalytic oxidation. Halogenated hydrocarbons are readily mineralized. Aromatic molecules are also quantitatively oxidized.

Chlorinated phenols, bisphenols, and even dioxins are also completely oxidized yielding CO_2 and HCl as final products. If the mineralization is not complete, some even more toxic byproducts could be released. This fact has been proven by Farley S. Braz et al. (2014) [8] and Natali-Sora (2016) [4] both studied the photodegradation of ibuprofen, the first using TiO_2 as photocatalyst and the second one working with a $LaFeO_3/H_2O_2$ system and visible

light irradiation. Therefore, the ecotoxicity test after the reactions are very important when the PCO technique is followed by a biological treatment or if the water will be directly discharged to the environment. The TOC (Total Organic Carbon) tests after a degradation reaction result very interesting to establish if the complete mineralization is achieved.

The mineralization of dyes, phthalates, DDT and surfactants has been reached. The research activity over the world is mostly devoted to the PCO of wastewaters containing refractory and toxic organics. However, PCO and other AOPs may play an important role in dealing with today's challenging demand for new water treatment technologies. The pH value has a dominant effect on the photocatalytic reaction because many properties, such as the semiconductor's surface state, the flat-band potential, the dissociation of organic contaminant, are all strongly pH dependent. The solution matrix can influence the photocatalytic reaction rate of a particular compound in several ways. One of the most studied and so more understood pollutant for the determination of the degradative effectiveness of TiO_2 is phenol. This molecule is used by the authors for the quality tests when a new TiO_2-based catalyst is synthetized. Weichgrebe [9] indicated that PCO is the best in terms of the process rate at pH 3.0 (pH 3.0, 5.0, 7.0, and 11.0 were tested) when landfill leachate is treated by either H_2O_2/UV or TiO_2/H_2O_2/UV. However, Way and Wan [10] found that acidic conditions with pH value less than 2 do not favor the PCO of phenol. The phenol degradation rate increases with increasing pH and has its maximum at pH ~6.5. As the

pH value increases further, the removal percentage diminishes rapidly. However, when the pH value is above 11, the phenol oxidation rate will increase again. Similar dependence of phenol decomposition on pH, although with some differences, was observed by other authors. In general, the optimum pH for the most effective PCO depends strongly on the character of the compound to be oxidized. Thus, aromatic amino compounds behave differently from phenol compounds. Experiments with tert-butanol, added as an $OH\cdot$ radical scavenger to the solutions of phenolic and aromatic amino compounds photocatalytically oxidized under different pH, showed that the radical oxidation mechanism prevails under alkaline medium conditions. Under acidic medium conditions, $OH\cdot$ radicals seem not to play a significant role in PCO [11].

Despite the proved effectiveness of titanium dioxide, its activation by the energy of UV irradiation is an important limitation for its effective commercialization, because of the costs and the health problems generated by this kind of illumination. Another disadvantage is the low exploitation of solar light, since only 4% of the solar radiation that arrives on the Earth surface is within the UV range. That's why the studies are focused on the modification of TiO_2 trying to render it sensitive in the visible spectrum, which represents nearly 50% of the solar irradiation reaching ground level. First the doping with transition metals was studied but the cost increases and the effectiveness decreases. Other studies are focused on the synthesis of TiO_2 doped with N or other non-metals or on its coupling with a narrow band gap semiconductor (M_xO_y/TiO_2, M_xS_y/TiO_2 or

$LaFeO_3/TiO_2$ [12]). Recently the use of a combination of the semiconductor and graphene had been reported; Xin Li et al. have presented an interesting review regarding the graphene-based heterojunction photocatalyst [13]. Other investigations concern the application of other semiconductors with lower band gap that are activated by the visible light irradiation such as lanthanum ferrite.

1.3 A visible light photocatalyst: $LaFeO_3$

The mixed oxide $LaFeO_3$ is a perovskite type compound with very interesting properties and application that will be shown below.

1.3.1 Perovskite type structure

These structures take the name from the mineral Perovskite ($CaTiO_3$) discovered by Gustave Rose in 1839. It was named after the Russian mineralogist Count Lev Aleksevich von Perovsky (1792-1856).

The general chemical formula for this crystal structure is ABX_3 where A is a cation larger than the cation B and the anion X bonds to both.

The ideal cubic-symmetry structure has the B cation in 6-fold coordination, enclosed by an octahedron of anions, and the A cation in 12-fold cuboctahedral coordination.

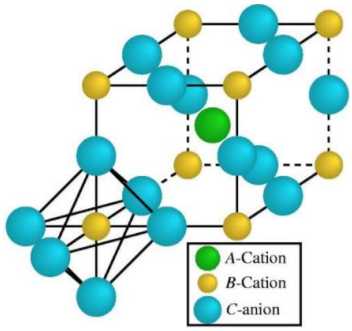

Figure 1.1: Perovskite type structure[1]

Many mixed oxides take perovskite structure (ABO_3). A is a rare or alkaline earth metal and B is a transition metal. The most common perovskite type mineral is bridgmanite ($(Mg,Fe)SiO_3$), other are loparite ($(Ce,Na,Ca)(Ti,Nb)O_3$), and the silicate perovskite ($CaSiO_3$)

1.3.2 Properties and applications

Perovskite materials show many interesting and intriguing properties; magnetoresistance, ferroelectricity, superconductivity, charge ordering, spin dependent transport, high thermopower and the interplay of structural, magnetic and transport properties are commonly observed features in this family. These compounds are used as sensors and catalyst electrodes in certain types of fuel cells [14] and are candidates for memory devices and spintronic applications.

[1]Source: *Julian Realpe on Oct 01, 2015*

These properties increase with the oxygen vacancies generated by the substitution of A or B metals.

$PbZrO_3$, $BaTiO_3$ and $PbTiO_3$ (used as piezoelectric compounds) $BiFeO_3$ (one of the most promising multiferroic materials), $LaMnO_3$, $YAlO_3$ (laser material), $SrTiO_3$ (radioisotope thermoelectric generator) are some of the most studied perovskite structures. Among these ternary oxides, lanthanum orthoferrite, $LaFeO_3$ (LF), is of great interest, not only for its use as high temperature material [15], but also for its possible application in a number of technologies such as solid-oxide in fuel cells [16], [2] sensor element for the detection of alcohol and humidity [17], catalyst in Fenton-like reactions [18] and photocatalyst.

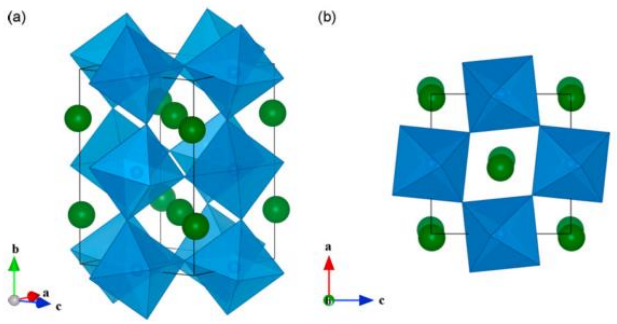

Figure 1.1 Crystal structure of $LaFeO_3$; a) unit cell of orthorhombic $LaFeO_3$ showing the inclined FeO_6 octahedral in blue, the lanthanum atoms in green are placed in the cavities between the octahedral, b) projection along the b-axis.

Comparing the degradation rate of acetic acid by perovskite supported on cordierite ($2MgO\ 2Al_2O_3\ 5SiO_2$) and on corundum

(Al_2O_3) honeycomb monolith [19], better results have been found with the latter support. The supportation was carried out by impregnation and applying a sol-gel synthesis. The same group [20] studied the degradation of methanol, acetaldehyde and oxalic acid by LF supported on corundum, resulting in 53, 62 and 95% of TOC reduction respectively. The lamps used for the irradiation were UV lamps emitting at 254 nm and no attention was given to the photocatalytic activity of lanthanum ferrite with visible light. In the same paper, it has been demonstrated that the result is worst if the oxidising agent is added just once at the beginning of the reaction, because of occurring H_2O_2 decomposition to O_2 that subtracts the oxidant to the photo-Fenton reaction.

Lanthanum ferrite-based materials have a great potential as photocatalyzers, thanks to their excellent properties such as their relatively small band gap, between 2.2 and 2.6 eV, stable structures and low cost. In this thesis, ferrite composites are reviewed as photocatalysts for self-cleaning surfaces and degradation of contaminants. Special attention is paid to the performance of these materials under visible light irradiation. The synergistic action of ferrites with common oxidants including hydrogen peroxide (H_2O_2), peroxymonosulfate (PMS), and peroxydisulfate (PDS) in decomposing pollutants is also addressed.

1.3.3 Photocatalytic properties

$LaFeO_3$ was proposed as visible-light photocatalyst in 2007 [21] by Li et al., who showed how its photocatalytic performances in degrading Rhodamine B under irradiation with $\lambda > 400$ nm were higher than those of TiO_2 (P25) in the same conditions. The annealing temperature reached during the material's synthesis was also studied, concluding that better degradation rates were achieved at 500 ºC, while poorer results were obtained when the calcination temperature increased. The first detailed study on the photocatalytic degradation of organic compounds was reported by Su et al. 2010 [22], who observed an excellent photocatalytic performance in Rhodamine B degradation in aqueous solution. Large surface area LF was prepared by a template method and the photodegradation rate increased, in these experiments, with the calcination temperature. Successive studies performed using nanostructured $LaFeO_3$ with different morphologies [23] confirmed its capability for visible-light degradation of Rhodamine B (RhB) and showed the morphological dependence of its photocatalytic performances. Three different shapes (cubes, rods and spheres) were synthesized by hydrothermal methods and subsequently tested.

Water decomposition by $LaFeO_3$ assisted by visible light was also studied in 2010 [24], using ethanol as a sacrificial electron donor to avoid the recombination process and without any co-catalyst, achieving after 180 min of irradiation production of 1290 μmol and 640 μmol respectively of H_2 and O_2. In 2012 [25] the use of Pt as co-

catalyst, electron transfer agent, allowed reaching 9945 μmol of H_2 after the same irradiation time.

Fenton-like reaction could enhance the photocatalytic degradation of Rhodamine B through a synergistic effect [26]. Little is known about the photocatalytic efficiency of $LaFeO_3$ under visible-light for the degradation of molecules other than the organic dyes. Recently, it has been reported that $LaFeO_3$ displayed photocatalytic activity for the degradation of ciprofloxacin (90 %) and ibuprofen (40 %) in water after 5 h visible-light irradiation [4].

Immobilization of $LaFeO_3$ to extend its surface area, increasing the number of active sites and allowing easier recycling, is being also investigated. A recent publication [27] showed how LF particles supported over carbon spheres enhanced the photocatalytic degradation of RhB. The reactions involved, in their opinion, are also reported:

$$LaFeO_3\left(Fe^{3+}(surf)\right) + H_2O \xrightarrow{h\nu} LaFeO_3(Fe^{3+}(surf)(h^+ + e^-)) + H_2O \longrightarrow LaFeO_3\left(Fe^{2+}(surf)\right) + {}^{\cdot}OH + H^+ \quad (1.1)$$

$$LaFeO_3\left(Fe^{2+}(surf)\right) + H_2O_2 \longrightarrow LaFeO_3\left(Fe^{3+}(surf)\right) + {}^{\cdot}OH + OH^- \quad (1.2)$$

$${}^{\cdot}OH + RdB \longrightarrow \cdots CO_2 + H_2O \quad (1.3)$$

This and other studies, where the heterogeneous Fenton-like (or photo Fenton-like) reactions are being investigated using $LaFeO_3$ as catalyst, report no leaching of iron in the solution, at least above the common detection limit of 5.0×10^{-3} mg/L in the Atomic Absorption Spectroscopy analysis. This is a guarantee that no homogeneous Fenton-like reactions are taking place and an interesting element confirming the possibility of photocatalyst recycling.

1.4 Photocatalytic coating materials.

Nowadays uses of TiO_2 as photocatalyst in building materials (concrete, mortar, paints, windows) are present in our cities to purify the air and to keep the surfaces clean, thus reducing maintenance requirement. Different construction elements have been already coated: buildings, roads and tunnels (with dedicated UV lighting system). Its self-cleaning performances are due to the redox reactions promoted by UV light (natural or artificial) on the surface catalyst. These reactions mineralize the organic molecules, so that the salts formed are cleaned away by the rain, and they also turn noxious organic and inorganic substances present in the air into harmless compounds.

To provide a guide to correct and recognized methods to evaluate the performances of these materials, ISO norms have been developed since 2007. ISO 22197-1: 2016 [28] specifies a test method for the determination of air purification performances of materials that contain a photocatalyst or have photocatalytic films on the surface, usually made from semiconducting metal oxides by continuous exposure of a sample to the model air pollutant under illumination with ultraviolet light. ISO 22197-2: 2011 [29] and ISO 22197-3: 2011 [30] are respectively the norms to follow for assessing the degradation of acetaldehyde and toluene. Also the self-cleaning performances are normed in ISO 27488:2009 [31] (water contact angle) and ISO 10678:2010 [32] (degradation of methylene blue in aqueous solution). The photosterilization characteristics are evaluated by ISO 27447:2009 [33]. Also the ultraviolet light sources

are tested in ISO 10677:2011 [34]. Visible light-sensitive photocatalysts are not included in any of these norms.

At the beginning this kind of coating was applied outdoor but when modifications were applied to TiO_2 to render it active with visible light irradiation [35], its indoor uses started to increase. Combination with other semiconductors with lower band gap or doping with metals first and non-metal more recently are some investigations conducted in this address. For indoor applications a new aspect has to be considered: byproducts generated by the photocatalytic degradation of the organic compounds of the paint, principally carbonyls: formaldehyde, acetaldehyde, propanal and acetone [36] that can be dangerous for the health if accumulated. This problem appears when the mineralization is not complete. The side products can be permanent and stable and can proceed also from the degradation of the air impurities [37].

CHAPTER 2 THESIS AIMS.

Lanthanum ferrite synthetized by our research group has interesting photocatalytic properties that could render it better than the traditional photocatalyst titanium dioxide for certain applications. To find and develop these potential applications it has been decided to explore the follow two fields:

_To employ $LaFeO_3$ in the preparation of a water-based photocatalytic paint, with low photocatalytic degradation effects on the components, because they are mainly inorganics, for outdoors/indoors applications. Accelerated ageing test were conducted to verify the stability of the coating under hard climate situations and photocatalytic studies were executed before and after the weathering test to study its self-cleaning properties durability. The paint natural ageing is being currently under study. The air purification was also studied with NOx degradation experiments.

_To support the catalyst on a ceramic foam for easier industrial applications of the already demonstrated water purification properties, avoiding the filtration difficulties and reducing the photocatalyst loss. Visible light photodegradation tests were carried out to compare its efficiency with the slurry tests.

The above tests and the need for scaling up led the research group to an increase in the production rate of the lanthanum ferrites. The

synthesis method used had been very well tested to produce small quantities (< 2 g) of $LaFeO_3$, in this work a new characterization is necessary because for the first time the amount of photocatalyst produced in a single batch has raised up to 12 grams. A complete characterization is presented, including FTIR, TGA, SEM, DRS and XRD analyses of three batches and their degradation performance to guarantee the quality of the product and the reproducibility of the synthesis method.

2.1 Self-cleaning approach. Photocatalytic paint

The effects of soiling on outdoor surfaces of buildings are well-known. Among the advanced protecting processes, coating with photocatalytic paint seems a very promising approach toward effective self-cleaning of the building facades. The photocatalytic process appears to be convenient and green in comparison with the traditional maintenance methods, reducing cleaning actions and costs, and retarding surface contamination. Commercial photocatalytic paints contain TiO_2 (anatase) as catalyst, which is activated by photons in the UV-A range for both the oxidation of organic substances and the inactivation of bacteria and viruses. The main applications of these paints are focused on exterior facades, which, via the photocatalytic processes, are maintained clean from organic pollutants and from the growth of microorganisms and fungi [38], [39]. Also, better air quality and reduction of smell in indoor areas can be reached with these paints.

This part of the thesis is focused on the photocatalytic self-cleaning properties of an innovative paint containing lanthanum ferrite photocatalyst (LF). Thanks to the low energy of its bandgap (between 2.2 and 2.6 eV), this semiconductor is active in the degradation of organic compounds under visible light radiation, namely more than the 40 % of the solar radiation reaching the Earth surface.

The traditional TiO_2-based photocatalytic paints can be applied over structures not exposed to sunlight, for example in tunnels, but they need UV lamps to be effective, so the LF paint would be more useful for the indoor surfaces.

A water-based paint was used, in order to minimize the organic material in contact with the photocatalyst. The main components of a water-based photocatalytic paint for outdoor surfaces of buildings are: pigments, mineral fillers, binder, and, of course, water. Minor additives are also present, such as dispersing agent, wetting agent, anti-foaming agent, rheological agent, thickener, coalescence agent and photocatalyst. Under irradiation the photocatalyst could photooxidise the polymer binder, and therefore loss of catalyst particles (photochalking) [40], [41] could take place. To overcome this problem, in this study a paint with inorganic silicate binder was used, and although; due to the requirements of use, a small part of organic binder is necessary, in the commercial paint used the organic binder is the indispensable minimum. In view of the above consideration, investigations were undertaken on painted samples exposed to accelerated ageing tests using a climatic chamber, which

simulated weathering agents: UV-A radiation, rainwater and conspicuous temperature and humidity variations.

The studies of photodegradation capability of the new paint were conducted by tainting the surfaces with an azo-dye (Procion Red PX-4B) and exposing it to visible light in a photoreactor for different intervals of time. All the tests were executed in parallel with the paint as such, without addition of the photocatalyst (reference paint). The color degradation of the tainting material onto the solid phase was followed by UV-Vis diffuse reflectance spectroscopy (DRS).

These tests were realized again after the ageing tests in order to investigate if the photocatalytic performances underwent any change. That is, relative durability and self-cleaning properties of paints containing $LaFeO_3$ were compared to those without catalyst.

An area of our laboratories facade was painted in May 2016 with five different types of paint: commercial photocatalytic paint (white TiO_2-based), white reference paint, LF paint (magnolia color) and a non-photocatalytic magnolia color paint. The aim was to follow the natural outdoor ageing of the photocatalytic paint and to test its self-cleaning properties.

The air-purification properties of the photocatalytic paint were analysed by the NO_x elimination tests.

2.2 Water purification by supported $LaFeO_3$

Different studies have been conducted using $LaFeO_3$ and its derivatives as photocatalyst in heterogeneous photocatalytic processes for the degradation of organic pollutants. One of the

problems found in industrial application of this degradation process regards the filtration phases necessary to reuse the catalyst. They are very expensive due to the energy cost and the loss of catalyst, so it seems very interesting to develop an effective deposition system to immobilize the photocatalyst onto an inert support.

In this thesis, the dip-coating deposition method was applied to the preparation of thin films of catalyst on the support surface. A ceramic foam has been chosen as inert support because of its structure and its mechanical resistance. To study the photoactivity of these thin films as well as their reusability the photodegradation reaction of 4-Nitrophenol was studied. The degradation rate was followed by HPLC analysis and TOC.

An innovative spin-foam reactor is proposed to increase the contact between the solution and the photocatalyst, and to improve the light distribution and to increase the flow of the aqueous solution into the porous structure of the foam.

The determination of the number of reuse cycles is also presented. When the foam was inactive different techniques were carried out trying to reactivate it. SEM observations was also carried out to determine the reason of the loss of activity.

CHAPTER 3 MATERIALS AND METHODS

3.1 Chemicals

Procion Red PX 4B

In order to choose the dye to stain the surface of the self-cleaning coating, different types and colors were initially tested (methylene blue, rhodamine and a yellow azo dye). The tests consisted of spotting a certain area of several substrates such as fibrocement (Figure 3.1) or glass with the colorants, exposing the taint to visible light irradiation and following the discoloration through the UV-Vis spectroscopy.

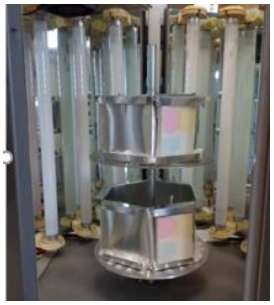

Figure 3.1 Preliminary studies to choose the model dye to determine the self-cleaning performances of the paint.

Procion Red PX 4B dyestuff (Figure 3.2) was selected for being the most stable to light, so the rate of degradation attributable to the action of the photocatalyst could be greater than the effects of direct

degradation. In literature [42], it has been already used for verifying substrate self-cleaning properties.

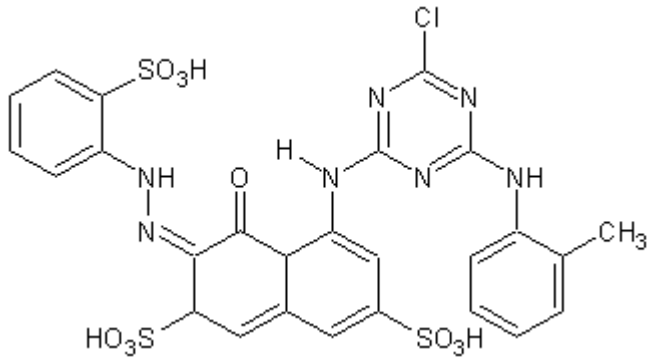

Figure 3.2 Procion Red PX 4B molecule [42]

Procion is a group of reactive dyes. These azo dyes were fabricated for the first time by Imperial Chemical Industries. The patent has expired and so different industries synthesize and sell them nowadays.

4-Nitrophenol

4-Nitrophenol is used as intermediate in the synthesis of drugs (acetaminophen), fungicides, methyl and parathion-insecticides, dyes and to darken leather. It is also used as pH indicator.

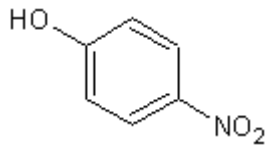

Figure 3.3 4-Nitrophenol

_Chemical formula: $C_6H_5NO_3$

_Molecular weight: 139.11 g/mol

_Melting point: 113ºC

_Boiling point: 279 ºC

_Solubility in water: 14.8 g/L

_Toxicity information: LC50 aq. (41 ppm (fishes, 96h))

Inhalation or ingestion causes headache, drowsiness, nausea, and blue color in lips, ears, and fingernails (cyanosis). Contact with eyes or skin causes irritation; it can be absorbed through skin to give same symptoms as for inhalation. Toxic oxides of nitrogen and fumes of unburned material may form in fires. It decomposes violently at 279°C and will burn even in absence of air.

It's a non-biodegradable substance that can be found in industrial waste water; it remains in the water even after the conventional treatments, causing environmental problems. Moreover, conventional treatments are expensive and can generate toxic intermediates. Advanced Oxidation Processes, and particularly heterogeneous catalysis [43] and photocatalysis [44], seem the most promising approach to degrade these molecules.

4-Nitrophenol is one of the more refractory aromatic contaminant found in some industrial waste water due to its high stability and solubility in water.

The Directive 2008/98/EC on waste is the Europe management law that establishes the waste hierarchy: prevention, re-uses, recycling, recovery for other purposes such as energy and disposal,

sentences the waste producer to pay for the costs of waste management. It also introduces the concept of extended producer responsibility, it makes a distinction between waste and by-products, waste management must be carried out without any risk to water, air, soil, plants or animals, producers or holders of waste must treat it themselves or have it handled by an officially recognized operator. Competent national authorities must establish waste management plans and waste prevention programs, special conditions apply to hazardous waste, waste oils and bio-waste. It introduces recycling and recovery targets to be achieved by 2020 for household waste (50 %) and construction and demolition waste (70%). This normative does not establish homogeneous standards for elimination of chemical waste like nitrophenols, therefore, its treatment depends on the internal regulation of each country.

This chemical was acquired from Aldrich and was >99 % pure.

Hydrogen peroxide (H_2O_2)

Used in this work as oxidizing agent for the pollutant degradation in combination with $LaFeO_3$; acquired from Panreac (30% w/v, 100 vol). In acidic solutions, it is widely used in AOPs as OH radical source, an oxidizing species strong enough to degrade organic contaminants present in the wastewater. Mainly used in the Fenton and photo Fenton reactions. It is considered an environmentally friendly reactant; anyway, the trend is to minimize the quantity added to the solutions in order to exhaust it at the end of the degradation reaction avoiding its leach to the environment and reducing the costs.

_Molecular weight: 34.01 g/mol

_Melting point: -0.43ºC

_Boiling point: 150.2 ºC

_Solubility in water: Miscible

_Viscosity 1.245 cP (20 ºC)

_Toxicity information: LC50 aq. (1418 ppm (rat, 4h)

There are authors reporting the formation of H_2O_2 directly from water by ultrasonication techniques [45], in this case the oxidation process is carried out without adding the reactant.

Other chemicals

All solvents, reagents and other chemicals were used as received, without any further purification.

3.2 Support materials

Fibrocement. This was the material chosen as support for the studies with the photocatalytic paint. A commercial fibrocement piece (4.0 x 4.0 m^2 and with a thickness of 0.8 cm) was acquired and platelets of 6.0 x 7.5 cm^2 were cut out with a handsaw for laboratory tests, degradation of taint and accelerated ageing test. The panel is usually used as prefabricated wall for outdoors requirements so it guaranteed resistance for the severe temperature and humidity conditions that it would suffer in the climatic chamber.

Ceramic Foam. The support employed for the deposition of lanthanum ferrite photocatalyst was a **c**ommercial ceramic foam filter called VUKOPOR® for foundry applications from "LANIK foam ceramics". Before use it was cleaned in an ethanol solution to

eliminate surface impurities. Its chemical composition declared by the fabricant is based on Al_2O_3 and SiO_2. The SEM analysis carried out on the foam in our laboratory shows that the molar ratio between them is approximately 5:2. In the micrography, the micro channels can be clearly observed, while in the photograph the microchannel of the foam are visible (Figure 3.4) of the blocks. Its maximum working temperature is 1350ºC, its porosity is 10 ppi (pores per inch), it is white and the dimensions of the blocks were 50 x 50 mm^2 with a thickness of 20 mm.

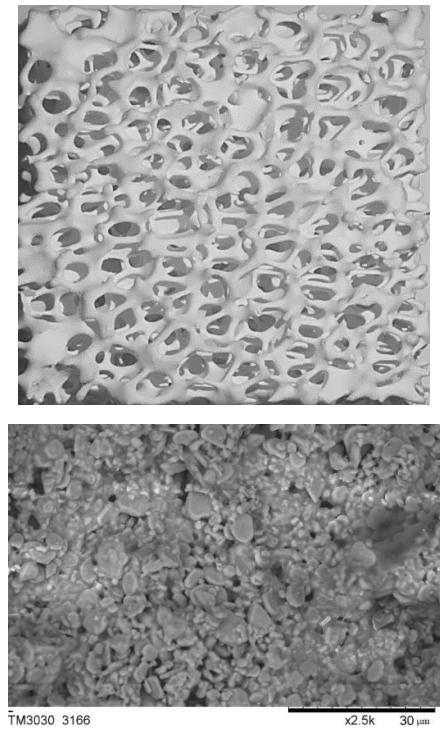

Figure 3.4 Photograph (above) and SEM micrograph (bottom) of the Al_2O_3/SiO_2 foam support.

3.3 Characterization techniques

3.3.1 X-Ray Diffractometry (XRD)

The crystalline phases and its crystallinity grade of the material were studied by XRD. The instrument employed was a Bruker D8 ADVANCE, the specimens were analysed with intervals of 2θ of 0.02º and the acquisition time was of 1 second for each point. The 2θ range of work was between 25 and 35 for the faster analysis and between 25 and 65 for the more complete ones.

3.3.2 Scanning Electron Microscopy (SEM)

The surface morphology and the composition of the samples were analysed by Scanning Electron Microscopy performed with a TM3030 Hitachi Tabletop furnished with a ray X dispersive energies detector EDAR for quantitative microanalyses. Scanning electron microscopy (SEM) observations were performed on the catalyst powders and the supported catalyst (photocatalytic paint supported onto fibrocement platelets and catalyst supported on ceramic foam)

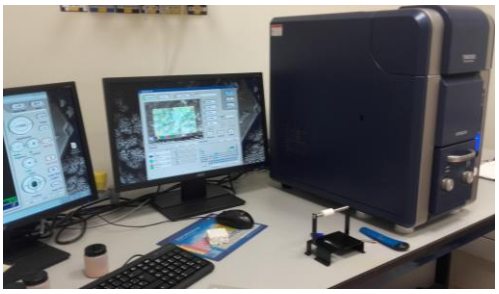

Figure 3.5 TM3030 Hitachi Tabletop (SEM)

3.3.3 Fourier Transform Infra-Red spectrometry (FTIR)

To characterize the photocatalytic powder and the photocatalytic paint before and after the ageing cycles Fourier Transform Infra-Red analysis (FTIR) spectroscopy was carried out with a Thermo Scientific Nicolet iS10 equipped with a KBr beam splitter and a DTGS detector. The spectra were collected in the range 400 - 4000 cm^{-1} at a resolution of 4 cm^{-1}, accumulating 50 scans.

3.3.4 Thermal Gravimetric Analysis (TGA)

A TGA model DSC 1 Star System from Mettler Toledo was used for thermogravimetric analysis. Simultaneous weight change and flow heat could be measurement with this instrument. Its high precision balance allows 1 μg weight loss measurements. The measurements can be carried out into different atmospheres (N_2, Air); for the test executed in this thesis air was chosen. The maximum investigated temperature was 1100 ºC.

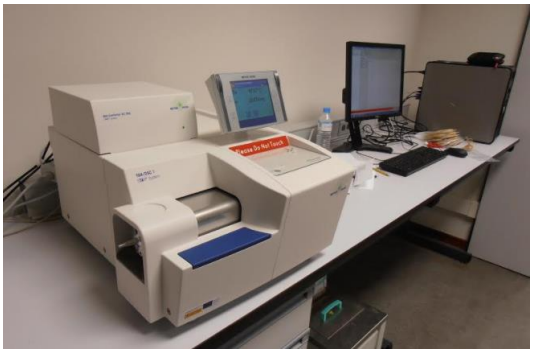

Figure 3.6 Thermal Gravimetric Analysis (TGA/DSC 1 Mettler Toledo Star System)

3.4 Analytical techniques

3.4.1 UV-Vis Diffuse Reflectance Spectrometry (DRS)

The DRS spectra for the first part of the present work (photocatalytic paint studies) were collected using an ultraviolet-visible (UV-Vis) spectrophotometer (Jasco V-650), equipped with a 60 mm integrating sphere (Figure 3.7).

Spectra of all samples were collected in four areas of the platelets before they were introduced in the climatic chamber or tainted in order to have four points for each sample to analyse the effect of the ageing cycles or to study the photodegradation performances respectively. The spectrum of untreated area (reference spectrum) was subtracted to all spectra.

Figure 3.7 UV-Vis Spectrometer JASCO V-650

A VARIAN spectrophotometer UV-Vis Model Cary 5 equipped with an integrating sphere was used for the band gap determination of the LF powders investigated in this thesis.

Kubelka-Munk (K-M) equations were used to transform reflectance data into absorption data [46]. Diffuse reflectance R of the sample was related to its absorption K and scattering characteristics S as in Eq (3.1):

$$\left(\frac{K}{S}\right) = \frac{(1-R_{\infty})^2}{2R_{\infty}} \tag{3.1}$$

3.4.2 High Performance Liquid Chromatography (HPLC)

To follow the concentration variations of the contaminant during the reactions in solution a High-Performance Liquid Chromatograph (HPLC) was employed. The Agilent 1260 Infinity instrument (Figure 3.8) with UV detector furnished with 8 diodes was equipped with a Supelco Discovery C18 (reverse phase) analytical column (250 mm×4.6 mm, packed with 5 μm particles)

Figure 3.8 HPLC 1260 Infinity (Agilent)

The flow rate was 1 mL/min for all the tests. The method used was:

_Mobile phase: 50:50 _0.005M KH_2PO_4 (pH 4.5 with H_3PO_4):H_3CN [47]

_Detection at λ=270 or 316 nm

_Response of 4-Nitrophenol with this conditions at 4.5 min for 270 nm and 4.7 min for 316 nm.

3.4.3 Total Organic Carbon analyser (TOC)

Once the rate of degradation of the pollutant was determined by HPLC, the level of mineralization achieved is studied because with the first information we only express the amount of contaminant that is degraded, but perhaps some byproducts remain in the solution, which could result even more toxic than the parent compound. One of the best techniques to obtain these data is the Total Organic Carbon analysis (TOC)

We studied the initial and final concentration for the most important reactions. The instrument used in this thesis was a Shimadzu model TOC-L (Figure 3.9) with an autosampler ASI-L Self-Sampler Shimadzu. This analyser determines the total carbon (TC) by a non-dispersive IR detector (NDIR) after oxidation to CO_2 by catalytic combustion at 680 ºC, using a Pt catalyst supported on carbonates. Inorganic carbon (IO) is obtained by the acidification of the sample with phosphoric acid, a process in which CO_2 is formed and detected by the NDIR. The TOC is established by difference

(TC-IC) or approaching the non-purgeable organic carbon (NPOC) to TOC (when there are non-volatile compounds). In this case, the NPOC is obtained from acidification of the sample to eliminate all the IC and a subsequent agitation to eliminate all the purgeable organic carbon.

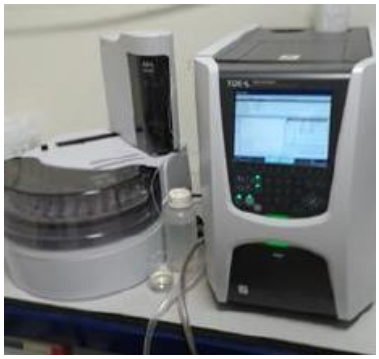

Figure 3.9 TOC Analyser. Shimadzu TOC-L

3.4.4 Atomic Absorption Spectrometry

Used for the iron detection in the solution resulting after the degradation of 4-Nitrophenol with the supported catalyst. The instrument was a Varian Techtron Pty Ltd. model AA-240FS Atomic Absorption Spectrometer equipped with a w/GTA-120 Graphite Furnace Accessory. The detection limit is of 5μg/L

The working conditions were: wavelength of 248.3 nm, pyrolysis temperature of 1000ºC, atomization temperature of 2300ºC, lamp intensity of 8.0 mA and tube with platform. The temperature profile is presented following:

Table 3.1 Temperature profile and injected volume. Atomic Absorption analysis.

I.V. (µL)	1 T/t (ºC/s)	2 T/t (ºC/s)	3 T/t (ºC/s)	4 T/t (ºC/s)	5 T/t (ºC/s)	6 T/t (ºC/s)	7 T/t (ºC/s)	8 T/t (ºC/s)	9 T/t (ºC/s)
20	85/5	120/35	140/15	1000/8	1000/10	1000/3	2300/0,8	2300/2	2300/3

Figure 3.10 Atomic Absorption Spectometer.

3.5 Catalyst synthesis: lanthanum ferrite (LF) and deposition method.

The catalyst was prepared in our laboratory by citrate auto-combustion method [1]. The precursors were analytical grade lanthanum oxide (La_2O_3), Ferric nitrate nonahydrate ($Fe(NO_3)_3 \cdot 9H_2O$), nitric acid (HNO_3), citric acid ($C_6H_8O_7$) and aqueous ammonia (NH_3). La_2O_3 was first annealed to eliminate the carbonate adsorbed by the oxide. Once decided the quantity of $LaFeO_3$ to synthesize, the necessary quantity of lanthanum oxide is dissolved in nitric acid to form $La(NO_3)_3 \cdot 6H_2O$. Then the ferric nitrate was added in stoichiometric quantity with respect to the lanthanum nitrate prepared. The concentration of this solution was 0.1 mol/L. A citric acid solution containing the necessary quantity of

acid to achieve a molar ratio 1:1 with metal ions was prepared. The first solution was added to the second and then aqueous NH_3 was dropped to increase the pH until 6.8, at this moment the solution became transparent. The solution is first dehydrated and afterwards heated in a hotplate to achieve the necessary temperature to autoignition. A brown powder, $LaFeO_3$, was obtained and annealed at 600ºC to eliminate any organic residues.

This synthesis method has been extensively tested for small batches of photocatalyst. In this thesis, for the first time, due to the intentions of scaling up and the high quantities required for the dip coating method used, large amounts of catalyst were prepared in each synthesis. That meant passing from 1 or 2 grams per batch in the traditional synthesis to 6 and even 12 grams per batch in the latest productions. This variation and the fact that some differences were observed between the different lots, led us to thoroughly test and characterize each batch.

After the calcination, part of the catalyst was ground in a mill. The procedure consisted of introducing 4 grams of LF in 20 mL of ethanol into a zirconium oxide grinding bowl with a stainless-steel casing with 124 zirconium oxide beads (5 mm). The bowl was inserted in the planetary mill that was set up with a speed of rotation of 700 rpm and ten cycles of 2 min of whirl and 1 minute pauses. So, the total time of milling was 30 min.

The planetary micro mill was a Fritsch Pulverisette Premium Line (Figure 3.11)

Figure 3.11 Fitsch Pulverisette 7 Premium Line and zirconium oxide grinding bowl with stainless casing

After grinding, the volume of ethanol was increased to 250 mL and the dip-coating process was started. The instrument used was a "Dip coater" KSV DX2S special for thin layer depositions. It has a mechanical arm that performs vertical movements with a programmed sequence introduced by a specific software.

The support employed was the ceramic foam described in 3.2.

A stainless-steel wire was introduced through the pores of the foam and held with the dip-coater clips. The sequence starts and the foam moves vertically inside and outside a beaker containing a suspension of catalyst in the continuously stirred solvent.

The substrate is immersed for 4 minutes to get an optimum contact between the catalyst and the foam. Then the withdrawing phase starts and the support raises slowly (50 ± 0.5 cm/min) and remains out of the suspension for 2 minutes, during which the film dries at atmospheric temperature. The descent speed was 10 ± 0.5 cm/min. It has been reported that low emersion speeds creates thin coats while high emersion speed forms inhomogeneous films due to the excess of liquid that remains on the substrate [48], [49].

Figure 3.12 "Dip coater" KSV DX2S.

Before the process, the suspensions were sonicated for 15 minutes to avoid particle agglomeration and to get a homogeneous dispersion of the catalyst into the solvent. The substrates were cleaned and degreased in ethanol.

Each immersion/emersion/standing sequence is considered as one cycle. Three, five and seven cycles were done in this work to establish the optimum number of these to get enough quantity of catalyst and homogeneous films over the foam. The catalyst concentration was 16 g/L.

At the end of the process the foams were calcined at 550 ºC for two hours (slope: 30 ºC/min). The final treatment consisted of washing the foams to eliminate the catalyst not correctly adhered to the surface. The $LaFeO_3$ loss were controlled by weight loss and by the turbidity of the washed water.

CHAPTER 4 CHARACTERIZATION OF THE PHOTOCATALYST ($LaFeO_3$)

4.1 Introduction

An exhaustive study of the catalyst for this thesis was developed, comparing the photodegradation capability of various $LaFeO_3$ batches synthetized by the same low temperature process and in high quantities. The synthesis reaction ends with calcination at 600ºC. The characterization of the lots evidenced some differences. These variations have some consequences for the degradation activity of the semiconductor, as we will see in Chapter 6.

SEM, FTIR, UV-Vis, XDR analysis and TGA measurements are shown here.

The batches studied were named Comb C8, Comb C10 and Comb C12-C13. It is necessary to remark that no variations were carried out in the synthesis parameters, the differences between them and with respect to the traditional productions (largely tested in our laboratory) were in the batch size.

Batch	Quantity synthetized (g)
Comb C8	6
Comb C10	6
Comb C12-C13	12

4.2 Scanning Electron Microscopy (SEM)

Here the results of the microanalysis of the different lanthanum ferrite powders are presented. The presence of nitrogen (N) is due to the nitrates remaining from the synthesis (See 3.5), coming from the ferric nitrate used as Fe^{3+} carrier or/and from the nitric acid used. The carbon (C) may come from the carbonate, present in the samples as will be shown in the next paragraph reporting on FTIR studies. It may derive both from the synthesis and from the atmosphere (CO_2). The easy carbonate formation by lanthanum ferrite is well known [50].
In Table 4.1 it can be seen the atomic percentage of the elements present in the photocatalyst and the ratio between lanthanum and iron and between oxygen and iron. The theoretical ratio La/Fe is 1 and O/Fe is 3.

Table 4.1 Micro-Analysis

Element	**La at. %**	**Fe at. %**	**O at. %**	**C at. %**	**N at. %**	$\frac{La}{Fe}$	$\frac{O}{Fe}$	$\frac{O}{La}$
Comb C8 (600°C)	18.34	18.00	52.67	7.72	3.26	1,02	2.93	2.87
Comb C10 (600°C)	16.94	15.96	53.56	9.96	3.59	1.06	3.36	3.16
Comb C12-C13 (600°C)	26.86	20.60	43.15	6.59	2.80	1.30	2.09	1.61

The products from the latter syntheses (C12/C13) show a significant oxygen vacancy. Surface oxygen vacancies enhance the

photocatalytic activity because they hinder charge recombination after the generation of electron-hole pairs by the irradiation energy. However, when the oxygen vacancy occurs in the bulk of the photocatalyst, the recombination of the electron and the hole is facilitated [51]. From the XRD analysis, a near 3% of La_2O_3 was found present in the C12/C13 powders but this presence doesn't explain the ratio La/Fe and O/La determined from the microanalysis.

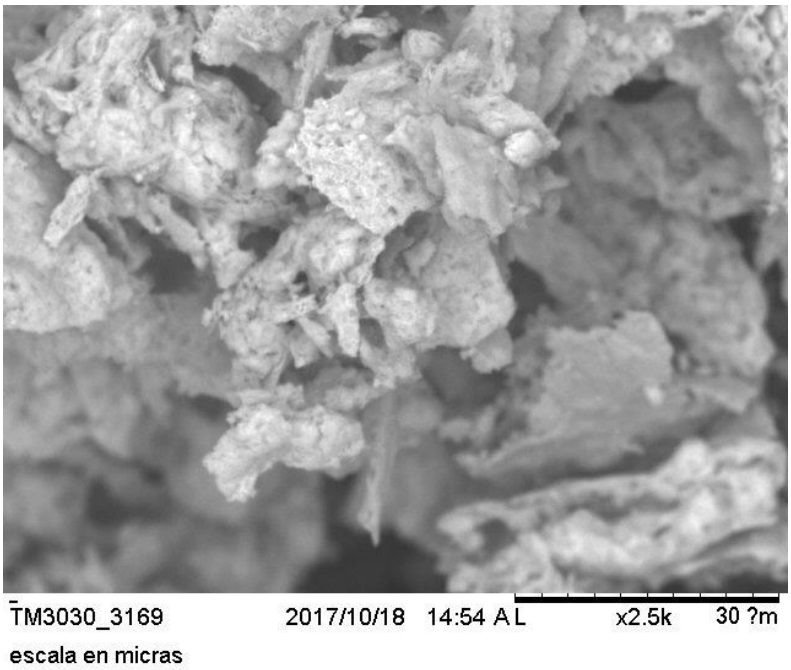

Figure 4.1 LF Comb C8 micrograph executed with a 2.5k optical magnification.

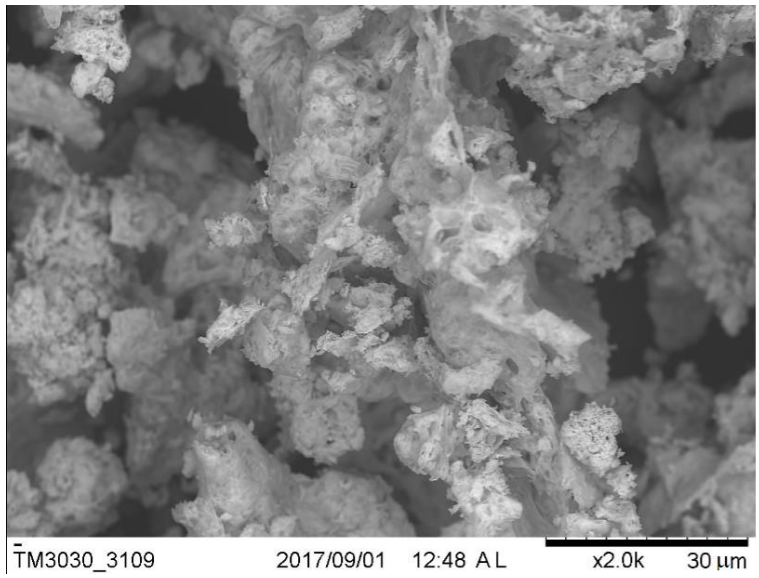

Figure 4.2 SEM micrograph LF C10 executed with a 2.0k optical magnification.

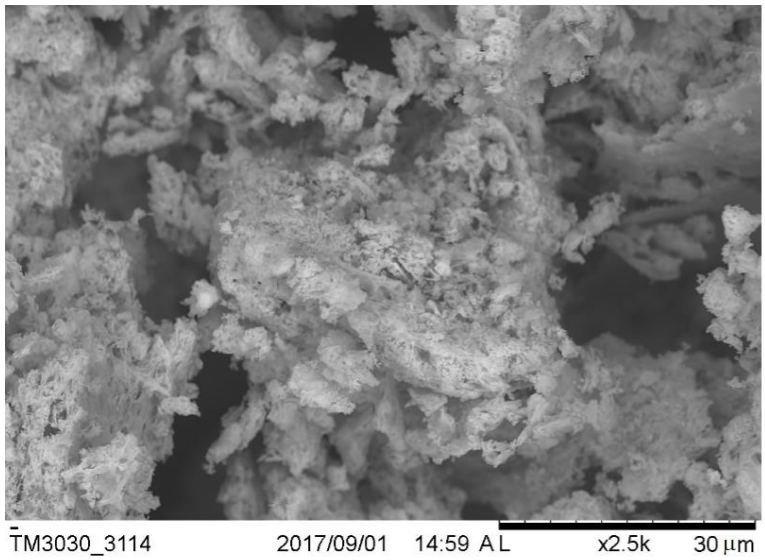

Figure 4.3 SEM micrograph LF Comb C12+C13 executed with a 2.5k optical magnification.

4.3 Fourier Transform Infra-Red Spectroscopy (FTIR)

From the FTIR spectra shown in Figure 4.4 several conclusions can be drawn. The baseline is significantly high for all the samples. The broad peak around 3450 cm^{-1} is due to the stretching mode of the hydroxyl group of bound water molecules, it's small in LF Comb C8 calcined at 600ºC and appears more intense when the sample is calcined at 900ºC for 2 hours, this fact was observed for all the batches. For the synthesis C10 this peak is inexistent and in the other cases the intensity seems similar. The presence of hydroxyl group in the surface of the semiconductor is important for the effectiveness of some photocatalytic reactions. The peak at 2350 cm^{-1} is due to ambient CO_2. Other two broad peaks can be appreciated: one around 1630 cm^{-1} that shows the presence of water and the other around 1380 cm^{-1} which is due to nitrates groups [52], [53] that is present in all the batches calcined at 600ºC while they disappear at 900ºC. Carbonate groups are observed in the three samples calcined at 600ºC the broad peak around 1480, is more intense for the C12+C13 batch. After calcination at 900ºC these bands are slightly displaced to around 1500 cm^{-1}.

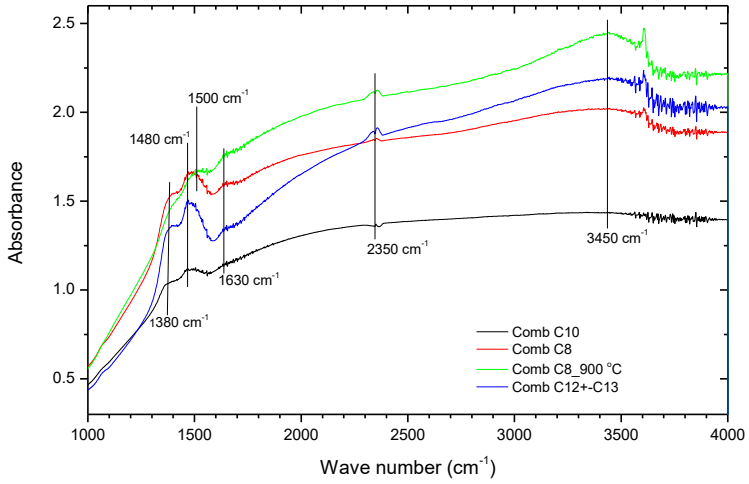

Figure 4.4 FTIR Studies of $LaFeO_3$ calcined at different temperatures.

The principal differences between the syntheses regard the intensity of the peaks, and in the case of the C10 sample, the absence of the peaks corresponding to adsorbed water molecules and hydroxyl groups.

4.4 UV-Vis spectra. Determination of Band Gap Energy

The forbidden energy gap values were determined based on UV-Vis diffuse reflectance spectroscopy measurements. The spectra obtained are presented in (Figure 4.5 A). The band gap energies were calculated through the first derivatives of these spectra as shown in (Figure 4.5 B). As it can be observed, there are two absorption edges,

the first corresponding to the ligand to metal charge transfer (LMCT) and the second one to the metal to metal charge transfer (MMCT). The Eg found for the $LaFeO_3$ powder was around 2.56 eV based on the direct transition in the situation MMCT, which is consistent with data reported elsewhere [3], [54], [55]

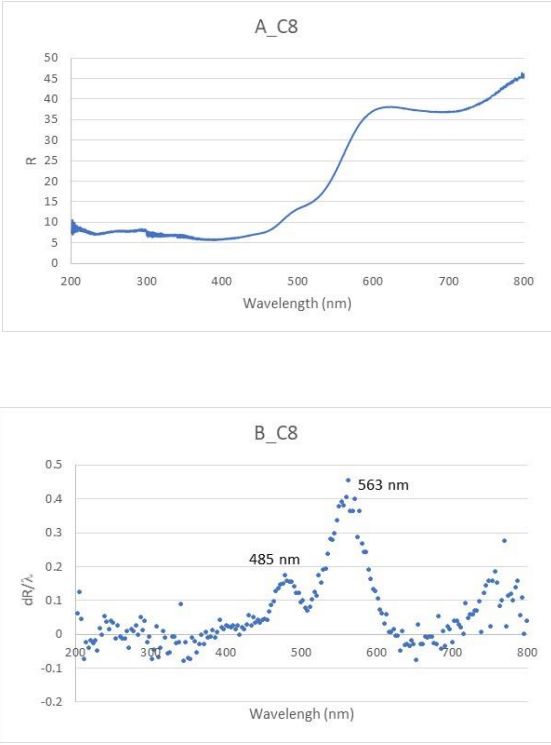

Figure 4.5 *A: UV-Vis Diffuse Reflectance Spectra and B: first derivative of the spectra for energy gap determination. C8*

The variations between the three analysed batches band gaps were negligible.

4.5 X- Ray Diffractometry (XRD)

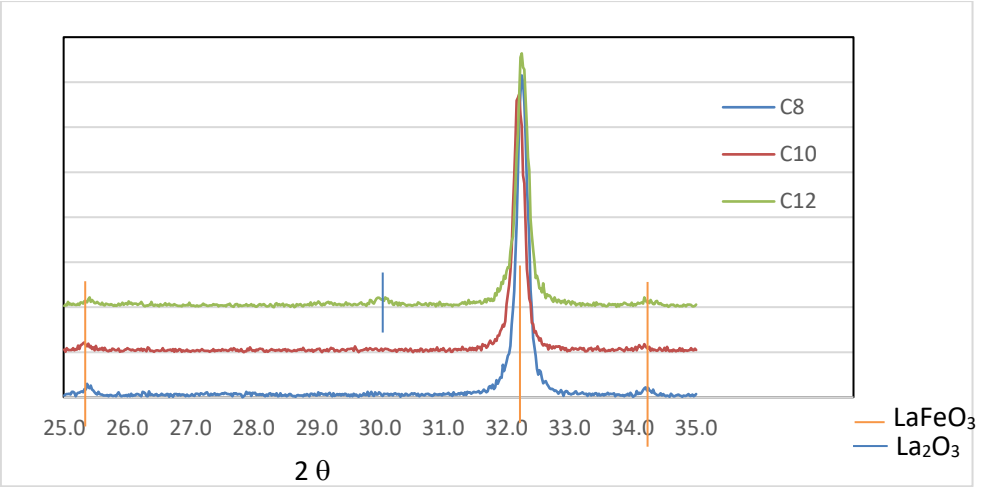

Figure 4.6 X- Ray Diffractograms of the three batches. Red vertical lines indicate $LaFeO_3$, blue vertical line indicates La_2O_3

Through this analysis the crystalline phases are appreciated. Only in C12 and C13 (C13 is not presented here) some La_2O_3 is present. This impurity can be estimated in less than 3 wt% of the total. The other two batches present only the peaks corresponding to $LaFeO_3$.

4.6 Thermo-Gravimetric Measurement (TG)

The thermogravimetric analysis Figure 4.7 of the three samples have been conducted after calcination at 600ºC. Considerable weight loss was observed up to 380°C followed by a slight weight loss in the 380–600°C range. A 0.27 % weight loss occurred between 650°C and 850ºC. The TG curves can be interpreted better based on FTIR studies (Figure 4.4) where peaks corresponding to nitrogen and carbonate bands appear.

The concentration of the impurities in the powder are slightly different as can be observed in the interval from 0ºC to 380ºC (1.7%, 1.3% and 1.0% for C12+C13, C8 and C10 respectively) and in the range between 380ºC and 650ºC (0.5%, 0.5% and 0.25% for C12+C13, C8 and C10 respectively) Weight loss between 650ºC and 850ºC is due to the carbonates groups. The batch Comb C8 presents an inflexion point at 750ºC while the other two batches at 700ºC. This difference can be attributed to a different composition or a change in the crystalline structure of the material.

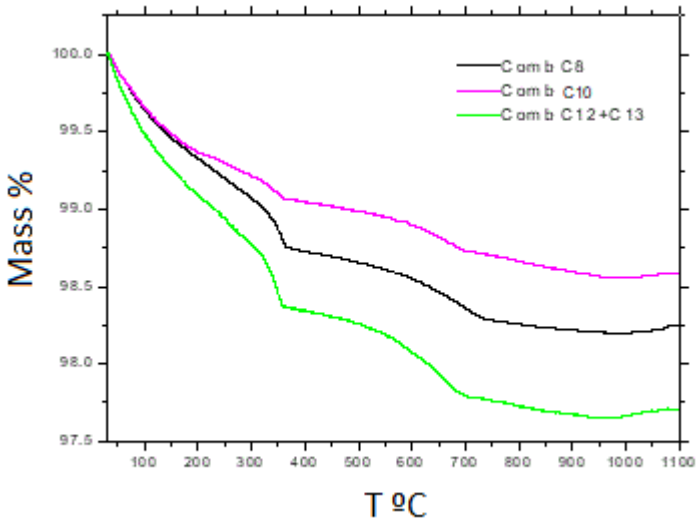

Figure 4.7 Thermogravimetric measurements

4.7 Conclusions

The aim of this part of the thesis was to evaluate if preparations of higher quantities of catalyst could have a negative impact in the quality of the final product. The batch size increased from 2 grams, the usual amount in past experiments, to 6 grams for the C8 and C10 batches, up to 12 grams in the case of C12 + C13. The characterization showed slight differences between the three batches. It is interesting to observe the differences and investigate whether they can have a consequence in the efficiency of the photocatalytic degradation. If so, the control during the synthesis phase must be increased. In this thesis some tests have been carried out in this sense, and it seems that their photocatalytic performances are almost the same. The last batch has more impurities, as can be seen in the TG analysis and through the XRD where even the presence of a La_2O_3 phase can be appreciated. This batch corresponds to the higher quantity ever synthetized in our lab, so more tests will be performed to clarify whether the reaction system must be modified for higher quantities.

CHAPTER 5 SELF-CLEANING PAINT

5.1 Introduction

A self-cleaning paint was prepared by the addition of $LaFeO_3$ to a commercial water based paint. The principal aim of this work has been to demonstrate that the addition of the photocatalyst to the commercial paint didn't cause an important loss of its performances. There are several works that describe the self-cleaning properties of a photocatalytic coatings [35]; less is known about how the photocatalytic particles can photo-oxidize the organic compounds of the paint [37].

Nowadays, self-cleaning commercial paints use titanium dioxide as photocatalyst. In this thesis, for the first time a paint has been prepared containing $LaFeO_3$, that needs only the energy of visible light irradiation to activate its photocatalytic properties.

5.2 Experimental

5.2.1 Samples preparation and characterization

Lanthanum ferrite $LaFeO_3$ was obtained by the citrate auto-combustion method [1]. The photocatalytic paint (LF) was prepared by mixing $LaFeO_3$ (1 wt%) to a commercial water-based paint. The decision to add only 1 wt.% of catalyst was taken because the percentages of the components of the two paints were maintained

very similar and the photocatalyst would not impact much on the price of paint. The paint (P) contained potassium silicate (SiO_2/K_2O) as inorganic binder, and, due to technical requirements to use, styrene-acrylic resin (5 wt%). It is possible, due to the type of degradation reaction carried out by the photocatalyst, explained in chapter 1, that the organic binder could be damaged, so that in this work a paint with the minimum amount of organic components in its composition has been chosen. Moreover, other main crystalline components were quartz (SiO_2) and calcite ($CaCO_3$) as mineral fillers, and rutile (TiO_2) as white pigment. It´s well known that the rutile phase of TiO_2 has no photocatalytic activity so the paint without $LaFeO_3$ lacks photocatalytic activity.

The phases composition of both paints was checked by using the XRD technique as can be seen in Figure 5.2. The second spectrum corresponds to the LF paint and the $LaFeO_3$ principal peaks are highlighted in red.

The color of the paint with LF was magnolia (a pale pink-orange tone), while the original was white.

Figure 5.1 Reference and photocatalytic paints on an external wall.

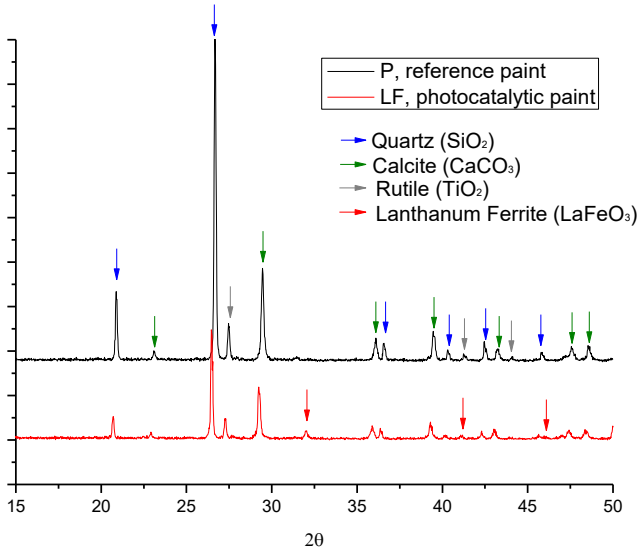

Figure 5.2 XRD spectra of the reference paint (P) and the photocatalytic paint (LF)

The paint was preserved under a thin film of distilled water to avoid the contact with the air present in the container. Just before use 40% w/w of distilled water was added and mixed with a magnetic stirrer, following instructions received from the manufacturer of the paint. Two layers of paint were applied to the surfaces of 6.0 x 7.5 cm^2 (8 mm thickness) fibrocement platelets using a brush. This turned out to be the best application system compared to the others that were tried. One of them was the spraying technique, with which very homogeneous surface areas were achieved but a low degradation rate was obtained in the preliminary degradation tests, concluding that too thin a layer was obtained with this coating method.

Some samples were coated with the reference paint, while the other half with the photocatalytic paint. The edge of the platelets that would be inserted in the climatic chamber for the weathering tests was sealed with silicone (Polymax cristal express-Bostik) to prevent the ingress of water, which could have caused swelling of the specimens through the weathering tests, or led to unwanted cracks in the support of the paint during the ice phase. One of the most important differences between our laboratory weathering test and the real outdoor conditions effects is the ratio between the border area and the painted exposed surface areas, much higher in the laboratory samples. Working with these edge areas sealed reduced the consequences of this difference.

5.2.2 Weathering tests

Some control samples were kept in a dry and dark environment, while the rest were introduced into a laboratory weathering chamber programmed to subject the specimens to adverse environmental conditions. The climatic chamber (Figure 5.3) was a Challenge from ACS. Two sub-cycles were used; one to simulate rain, freezing, dry heat and humid heat, the second to carry out UV irradiation using a high-pressure Hg lamp (125 W, λ_{max} = 365 nm). In Table 5.1 the experimental conditions associated with each phase are listed. Three specimens of each type (LF and P) were extracted after 10 and 30 ageing cycles and twelve after 50 cycles, corresponding to 62 h, 185 h and 308 h of weathering tests, respectively. All specimens were

subsequently analysed by UV-Vis diffuse reflectance spectrometry and some of them by Scanning Electron Microscopy (SEM)

Figure 5.3 Weathering chamber with samples before starting the last 20 cycles.

Table 5.1: Experimental conditions of the weathering cycles

Sub-cycle A					
n°	Phase	T_{air} [°C]	T_{water} [°C]	RH [%]	Duration [min.]
1	Rain	20	15-20	…	60
2	Ice	-20	…	…	90
3	Humid heat	55	…	95	60
4	Dry heat without UV	70	…	40	80
Sub-cycle B					
n°	Phase	T_{air} [°C]	T_{water} [°C]	RH [%]	Duration [min.]
1	UV Radiation	30	…	40	80

Once the desired conditions are set in the chamber software, the cycle starts and the temperature and the relative humidity are continuously controlled and registered. Figure 5.4 shows a graphic

representation of the real conditions and the settings during the execution of one of the sub-cycles A.

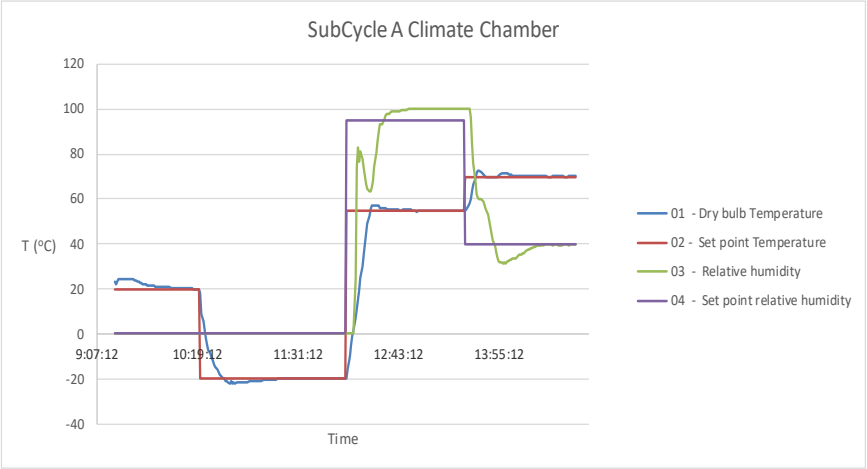

Figure 5.4 Example of temperature and humidity control carried out during a sub-cycle A

The climatic chamber is usually used to define the reference service life of the construction elements. The setup of the machine obviously depends on the weather conditions of the place where the material will be placed. The research group at Politecnico di Milano who provided the climate chamber for the test [56] has previously established these cycles as representative of the climatic conditions of Lombardy. To determine the temperature, rain, humidity, UV radiation and the duration of each phase, the extreme weather conditions of a representative year are considered and the mild ones eliminated. Concretely, the 50 cycles employed for this thesis

correspond approximately to two years of natural exposition in the region of Lombardy.

5.2.3 Photocatalytic self-cleaning tests

For the evaluation of the photocatalytic self-cleaning properties, the color degradation of an azo-dye (Procion Red PX-4B, (Dyestar, Italy)) onto the paint surface on the platelets was monitored after regular intervals of light irradiation. $LaFeO_3$ is a semiconductor with band gap energy in the range of 2.2-2.6 eV [3], [57], thus the photocatalytic color degradation reaction was carried out in a photoreactor (Multirays) equipped with 10 lamps (8 W, Daylight) emitting in the visible region (Figure 5.5). The specimens were placed in an ad-hoc prepared support that rotated about a central axis in order to ensure even exposure to radiation.

Figure 5.5 Photoreactor (Multirays) and ad-hoc prepared support with the specimens

The dye solution was prepared in a 90:10 (v:v) mixture of acetone and water. The decision to use only a 10 % of water was due

to the requirement of fast solvent evaporation to obtain a stain as homogeneous as possible on the surfaces studied. The dye concentration was 0.4 g/L. The specimens were tainted by dropping a fixed amount of the dye solution onto the paint surface, then they were left 48 h in the dark to allow a complete evaporation of the solvents before starting the self-cleaning test. Table 5.2 summarizes the experimental conditions of the samples tested for self-cleaning properties.

Table 5.2: Experimental conditions of the samples tested for self-cleaning properties. Weathered samples are labeled by W

Reference samples	Weathering cycles	Vis-light irradiation (h)	Photocatalytic samples	LF (wt%)	Weathering cycles	Vis-light irradiation (h)
P	0	0	LF	1	0	0
P1	0	120	LF1	1	0	120
P2	0	240	LF2	1	0	240
P3	0	360	LF3	1	0	360
PW	50	0	LFW	1	50	0
PW1	50	120	LFW1	1	50	120
PW2	50	240	LFW2	1	50	240
PW3	50	360	LFW3	1	50	360

The color degradation of the dye on the paint layer was followed in solid phase by diffuse reflectance spectrometry (DRS). The Kubelka-Munk (K-M) [46] equations were used to transform the reflectance data into the absorption data (see paragraph 3.4.1).

The dye photodegradation percentage of the Procion Red PX-4B azo-dye was calculated from the absorption intensity data at the λ_{max}

= 551 nm for all the LF and LFW series, and λ_{max} = 548 nm for all the P and PW series using the equation (5.1)

$$Dye\ Photodegradation\ (\%) = \left(1 - \frac{D_t}{D_0}\right) \times 100 \quad (5.1)$$

where $D_0 = \left(\frac{K}{S}\right)_0 - \left(\frac{K}{S}\right)_p$, and $\left(\frac{K}{S}\right)_p$ was the K-M value of the untainted paint, while $\left(\frac{K}{S}\right)_0$ was the K-M value of the dye before exposure to the visible-light irradiation. Correspondingly, $D_t = \left(\frac{K}{S}\right)_t - \left(\frac{K}{S}\right)_p$ where $\left(\frac{K}{S}\right)_t$ was the K-M value after irradiation to t = 120, 240 and 360 h. For each sample, the measurements were performed on two different tainted regions.

5.3 Results and Discussion

5.3.1 Microstructural characterization of paint coatings

The paint surface on the specimens (LFW and PW series) subjected to the first 30 cycles showed a small bulging. The damage slightly increased with further weathering cycles (Figure 5.6), since the content of resin in the paint film was only 5 wt%, and as a consequence the film exhibited a permeability to water vapour. The water vapour condensed under the film, but in the weathering chamber during the dry heat phase it evaporated generating bubbles.

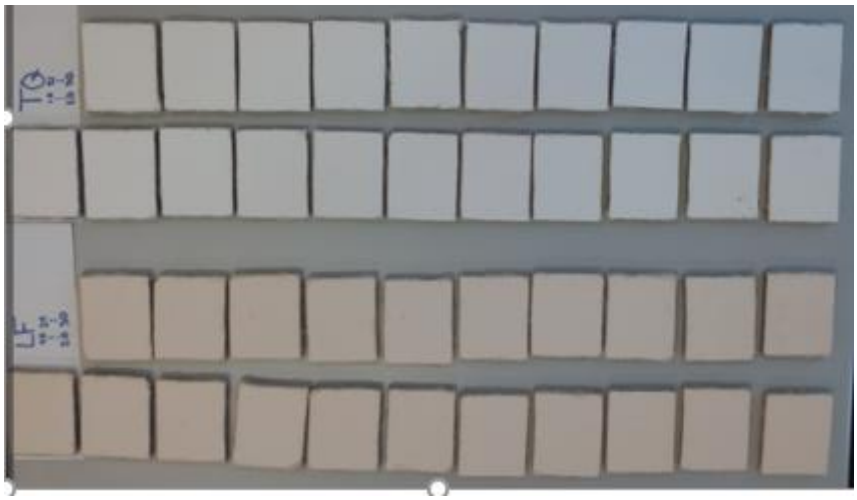

Figure 5.6 Platelets after the weathering cycles.

The results are in agreement with a recent study, which reported how weathering may influence the durability of silicate-based paint [41].

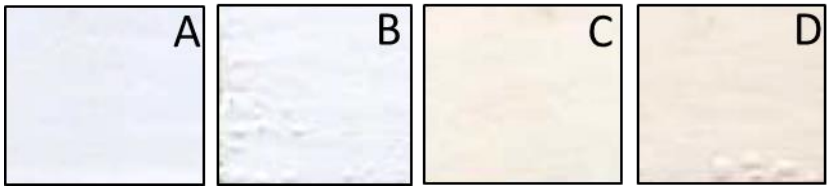

Figure 5.7 Images of A) unweathered P reference paint*; B) 50 cycles weathered PW reference paint, C) unweathered LF photocatalytic paint; D) 50 cycles weathered LFW photocatalytic paint.*

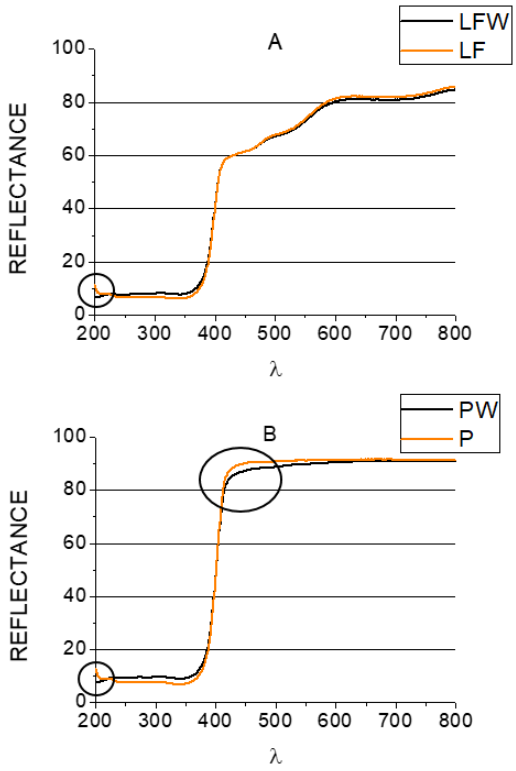

Figure 5.8: Spectra UV-Vis of the platelets; A) Photocatalytic paint: weathered (LFW, 50 cycles) and un-weathered (LF), B) Reference paint: weathered (PW, 50 cycles) and un-weathered (P)

The UV-Vis spectra show some variations between the samples before and after the ageing cycles. In Figure 5.8 the differences are marked with circles. All the samples started to present a slight reflectance values diminution at 200 nm of wavelength after the first 30 cycles; the variation increased after the 50 cycles. Tests developed in the laboratory in which other set of painted platelets were

submitted to UV irradiation in the Rayonet photoreactor gave the same differences in the spectra after 12 hours. From that it can be concluded that the damage is a consequence of the UV irradiation phase (sub-cycle B) and probably due to a degradation of the resin of the paint. This kind of damage, the same for both photocatalytic and reference paints, does not occur when the paint is irradiated with visible light. Only the reference paint has another difference around 420 nm. In that zone, it displays a diminution of the reflectance due to an increase of the yellow tone of its surface. This fact can be seen even to a naked eye since the first 30 cycles of ageing. The LF paint color seems do not suffer any change but it should be remembered that its initial color is different from the reference paint, $LaFeO_3$ gives it a magnolia tone.

SEM observations evidenced that the surface of the weathered samples (LFW and PW) showed slight pitting compared to the unweathered ones. SiO_2 phase showed to be present in two morphologies: a porous structure due to nanocrystalline silicate binder and large crystalline particles. Moreover, backscattered electron images (BSE) were used for rapid discrimination of phases in the samples. The distribution of "brighter" BSE intensity (correlated with the $LaFeO_3$ photocatalyst) were very similar in LF and LFW series indicating not significant loss of catalyst particles in the weathered paints. On the contrary, Si-map of LFW was poorer of the Si element respect to LF. The weathering treatments increased the roughness of the surface of both paints, which is supposed to be due to some loss of the silicate.

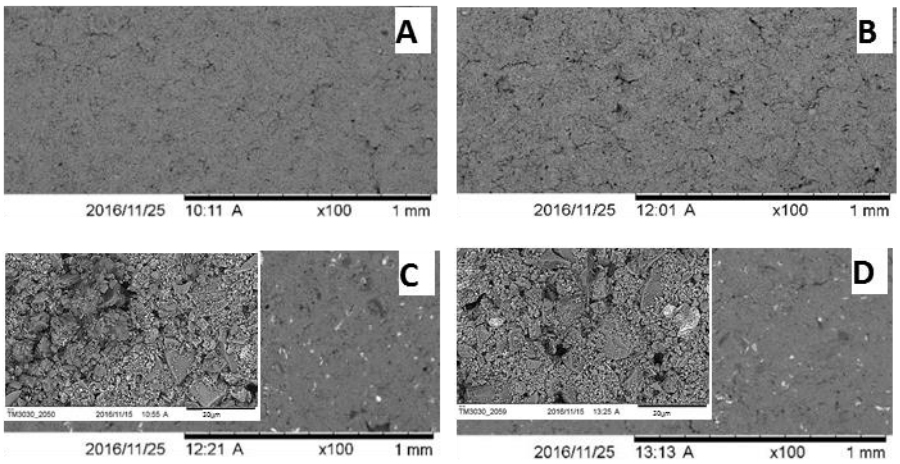

Figure 5.9: SEM micrographs of A) unweathered P reference paint, B) 50 cycles weathered PW reference paint; C) unweathered LF photocatalytic paint; D) 50 cycles weathered LFW photocatalytic paint.

The FTIR spectra of LF and LFW were similar but with some exceptions: differences can be noticed in the broad peak at ca. 1082 cm^{-1} corresponding to the asymmetric stretching of Si-O-Si overlapping the Si-O-K band vibrations, and in the broad carbonate multiple peak at 1400-1520 cm^{-1}. The silicate peak was stronger for unweathered LF paint, in agreement with the fact that the LFW coating has lost a small fraction of surface silicate. The carbonate peak is also slightly stronger for the LF unweathered sample. The weak peak at 1736 cm^{-1} was assigned to the carbonyl (C=O) stretching vibration. The fact that this latter peak, which is

characteristic of the styrene-modified acrylic resin spectrum [58], was identical in both (LF and LFW) indicates that the nature of the resin was not modified by the weathering tests.

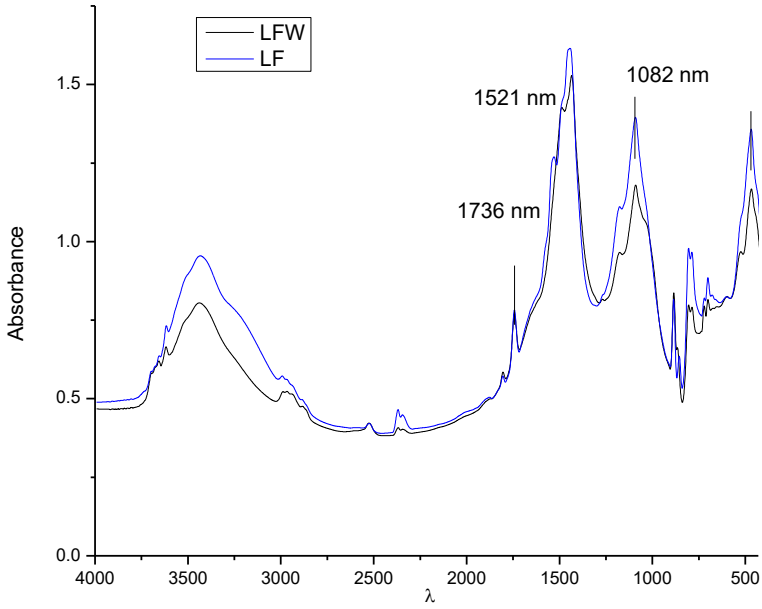

Figure 5.10: FTIR Spectra of the photocatalytic paint; LF non-weathered paint and LFW 50 cycles weathering one.

5.3.2 Photocatalytic self-cleaning results

The self-cleaning tests were done in parallel using reference and photocatalytic paints, in order to validate the reproducibility of LF catalytic behavior. Similar tests were conducted before the weathering test to check the photocatalytic properties of the prepared paint. The supports chosen for the preliminary test (

Figure 5.11) were slides and fibrocement platelets, this latter material was the one chosen for the tests in the climate chamber. The achieved results were interesting and promising. These tests were conducted with irradiation times of 6, 12 and 18 hours for the firsts tests, and of 120 and 240 hours, with other platelets. Observing that more important differences between both paint types appeared after longer irradiation times, we decided to perform tests with 120, 240 and 360 hours of light exposure periods for evaluating the platelets self-cleaning performances after the accelerated ageing tests.

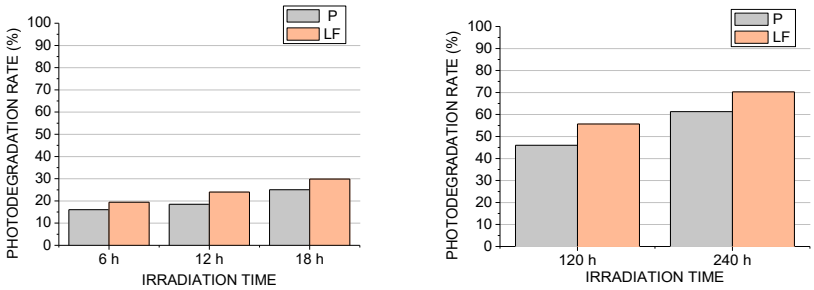

Figure 5.11 Preliminary tests. LF, photocatalytic paint, and P, reference paint on fibrocement. Left, the first test for short time intervals; right, the second tests for longer time intervals.

Test after accelerated ageing

The dye degradation percentage of Procion Red PX-4B using non-weathered paint (LF) under visible-light irradiation (360 h) was 78 %. The discoloration percentage of samples LF1, LF2 and LF3 were always higher compared to the reference P1, P2 and P3 samples, the difference in degradation percentage was constant at longer

irradiation times with visible light. After 360 h of visible irradiation, the dye with LFW3 paint displayed a dye degradation percentage of 67 % (Figure 5.12). Also in this case the dye discoloration of samples LFW1, LFW2 and LFW3 was always higher compared to the reference PW1, PW2 and PW3 samples, and the difference in degradation percentage was unchanging with longer irradiation time. Photocatalytic tests performed in aqueous solution with powder slurries as catalyst guarantee a continuous contact between the target molecules and the nanoparticles of the catalyst. In our case, the photodegradation experiments were carried out using LF in the solid paint matrix. This experimental configuration did not guarantee high accessibility of the catalyst at the dye molecules. Moreover, in this case the amount of catalyst was small (1 wt%), the contribution arising from direct photolysis of the dye was the most important after long irradiation time (360 h). The difference in the percentage of degradation between P and LF specimens was, in our opinion, due to the presence of the photocatalyst. The action of the photocatalyst is predominant during the first 18 hours of irradiations, after that moment the direct degradation plays the more important role.

The partial loss of nanocrystalline silicate and the consequent surface roughness modification, induced by the exposure of silicate binder to extreme experimental conditions in the climatic chamber may cause the decrease of the self-cleaning performances in the weathered samples. In fact, the slight increase in the superficial amount of acrylic resin which didn’t present the hydrophilic and porous nature of the potassium silicate prevented a homogeneous

distribution of the dye solution onto the paint films. Moreover, as described in section 5.3.1 BSE images indicated negligible loss of catalyst particles in the weathered paints. The lowering of the self-cleaning efficiency is not due to loss of catalyst, but to a microstructural variation of the paint surface.

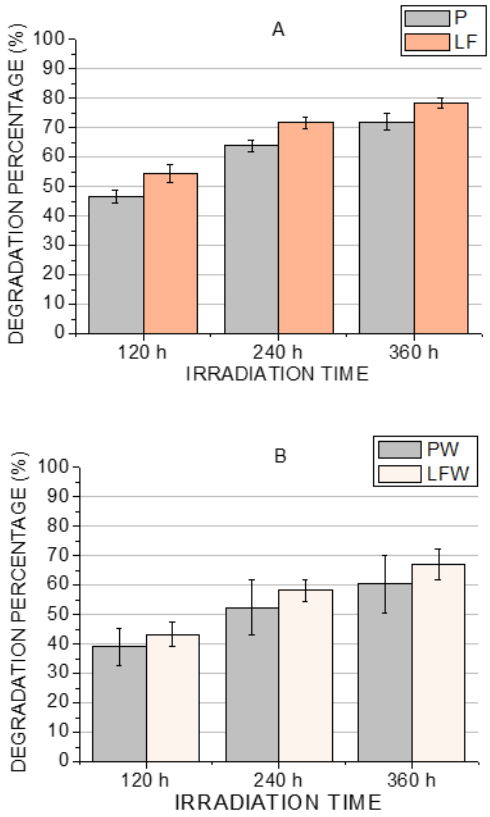

Figure 5.12 Photocatalytic dye degradation percentage of Procion Red PX-4B after 120, 240, 360 h visible light irradiation in A) unweathered samples, B) weathered samples.

Comparing the results obtained in the preliminary test

Figure 5.11), with the last ones, it can be said that they are highly repeatable and reliable.

5.4 Outdoor tests

After realizing the preliminary study of the $LaFeO_3$-based photocatalytic paint resistance to extreme weather conditions in the climatic chamber, a very important test was initiated, aimed to the monitoring of the conservation state of the paint when exposed to natural ageing. Three small areas of a facade were coated with various types of paint to compare its self-cleaning properties and other characteristics over time. The orientation of the wall is towards the south and it is located near a metallurgic industry.

The control of this wall was executed by photography. The wall remained clean in all the painted areas during the first year of exposition, it will take more time to appreciate the differences. The durability of the LF paint seems to be the same of the commercial paint, the addition of the photocatalyst did not reduce the commercial paint performances.

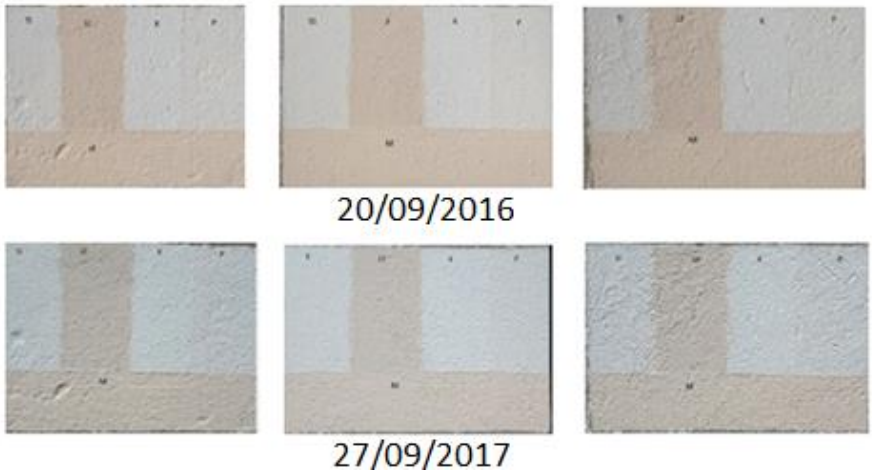

Figure 5.13: Photographs of the three small areas coated with the five types of paint (Ti, LF, K, P and M). The top three correspond to the initial moment and the bottom three portray the areas after one year of nature exposure.

The paints in study are: the reference paint with a 1 wt% addition of TiO_2 anatase (Ti), the $LaFeO_3$-based photocatalytic paint (LF), a commercial photocatalytic paint (Keim, k), the reference paint (P), and a magnolia color non-photocatalytic paint (M).

5.5 Air purification tests

For the determination of the air purification capability of the paint the NO_x degradation has been analysed.

The experiment was carried out following the standard UNE-ISO 22197-1 (*ISO 22197-1:2007*). The desired NO_x concentration was obtained from the dilution with air of a 100 ppm NO bottle (Air Liquide) through mass flow controllers (BRONKHORST HI-TEC,

model F-201CV-AGD-11-V). After the dilution into the mixture chamber, the gas is passed through the reactor (Figure 5.14).

Total flow rate was of 1.2 L/min. Tests were carried out for 5 hours, all of them preceded by 30 min of adsorption in the dark. The radiation was applied with the visible light lamps OSRAM DULUX L BLUE (see spectrum in Figure 6.2).

The flow reactor used to determine the air purification capability of the fibre cement platelets is showed in Figure 5.15. The effective volume in the reactor was of $26 \cdot 10^{-3}$ L and the gas regime was turbulent. The residence time was 1.29 seconds. The relative humidity was of 65%. The entries and exits were divided in three to ensure the gas flow over all surface of the specimen.

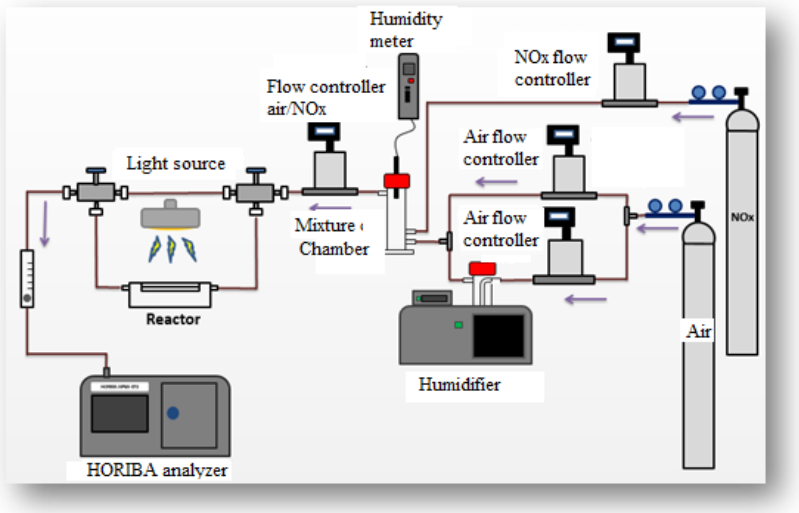

Figure 5.14 Scheme for the NO_x degradation tests.

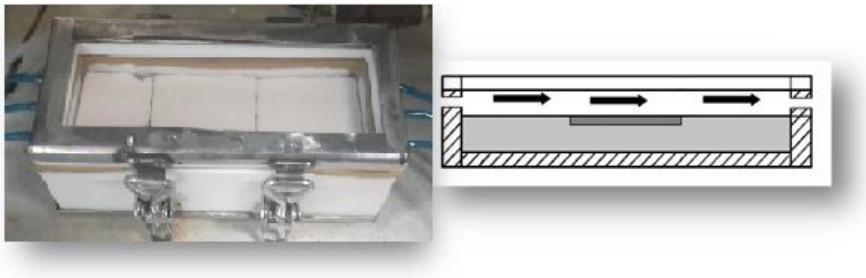

Figure 5.15 Scheme and photograph of the reactor with the photocatalytic platelets inside during the reaction

The NO_x determination was done by means of a HORIBA analyser APNA-370 N/S model. No NO_x degradation was observed during the reaction time as can be appreciated in Figure 5.16.

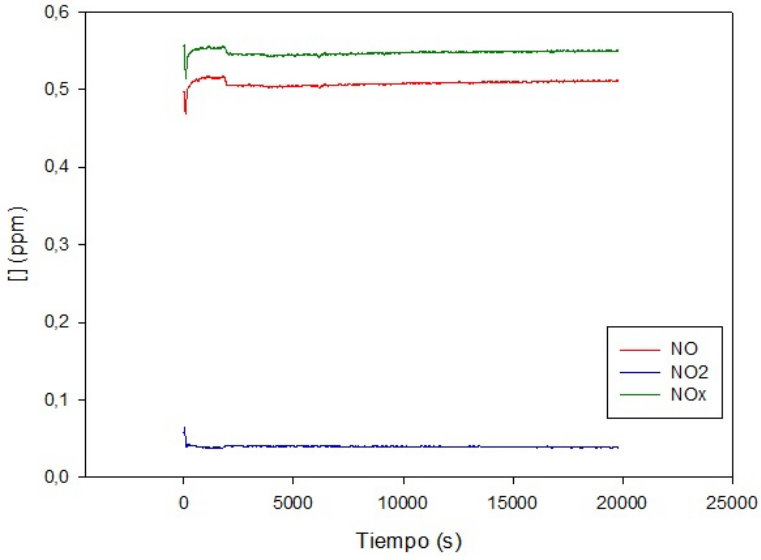

Figure 5.16 NO_x elimination test evolution. No activity was observed for the LF paint.

5.6 Conclusions

Water-based silicate-acrylic paint (reference paint) with the addition of 1 wt% of $LaFeO_3$ catalyst was tested for color degradation under visible-light irradiation of the Procion Red PX-4B azo-dye. The results were good and so it was decided to study possible negative impact of the modification introduced in the recipe of the paint with regard to the ageing process. Some samples of both photocatalytic and reference paints were exposed to accelerated weathering tests in a climatic chamber. The platelets were extracted after 10, 30 and 50 weathering cycles and analysed, showing the same type of damage in all of them, thus clearing the first point: the paint quality did not suffer any change with the addition of $LaFeO_3$. After that, the second aim of the present study was to determine whether the photocatalytic activity continued after the ageing tests, so the photocatalytic paint could resist the outdoor conditions. Tests conducted in parallel with both weathered and unweathered samples of photocatalytic and reference paints were carried out, following the degradation rate of the Procion red dye under irradiation with visible light through their UV-Vis spectra. A decrease in self-cleaning properties was observed due, in our opinion, to some loss of the silicate induced by the treatments in the climatic chamber. The color degradation of the photocatalytic paint was higher than that of the corresponding reference paint, both in weathered and unweathered conditions.

No NO_x degradation was verified during the experiments when using only 1% $LaFeO_3$ in the paint; the possibility could be explored that a higher amount of photocatalyst be effective in this reaction. However, increasing this amount could have adverse effect on both the price and durability of the paint. The paint might therefore not be the system of choice for the air depollution with this catalyst

The addition of 1 wt% of catalyst in economic terms did not impact much on the price of paint.

In order to obtain conclusions from outdoor tests at least one more year will be necessary.

CHAPTER 6 CATALYST DEPOSITION ON CERAMIC FOAMS

6.1 Introduction

Due to the expense involved in separation of nano-sized catalysts particles from treated water and the difficulties in terms of photocatalyst reutilization, there has been a growing interest in immobilization of the photocatalyst on inert solid supports.

However, supported photo-catalysts have been mainly described for the treatment of emerging pollutants or low pollutant concentrations. This is because when the catalyst is immobilized, there is an inherent decrease in the surface area available for reaction and consequently the reaction rates are lower. The porous supports that have been studied in this thesis try to avoid this problem, although the support may introduce interfering species into the photocatalytic system.

The process studied is a photocatalytic reaction; when $LaFeO_3$ is irradiated by visible light, electron-hole pairs are generated causing strong redox reactions on its surface that are able to degrade organic compound like 4-Nitrophenol. This reaction is enhanced when H_2O_2 is added by the synergistic effect between a Fenton-like reaction and the photocatalytic process.

6.2 Experimental

The first part of the work consisted in studying photo-degradation conditions with slurry photocatalyst to optimize irradiation times and pH values for the degradation of 4-Nitrophenol, and to obtain results to be compared with those achieved with the supported photocatalyst. As explained in the introduction, the main advantage of lanthanum ferrite photocatalyst is that it works with visible light irradiation, so the lamps used emitted in this range.

6.2.1 Illumination devices

In the laboratory test, the irradiation was applied with two different lamps: A Philips lamp SOLARIUM HB 175 model equipped with four 8 W fluorescence T5 tubes for common illumination and a OSRAM DULUX L BLUE 18/W/75 a specific lamp for laboratory uses.

Both spectra are shown in Figure 6.1 and Figure 6.2 and their principal characteristics are present in Table 6.1. These data were obtained by a spectro-radiometer from Ocean Optics (HR2000) in the laboratory at the beginning of the test sets.

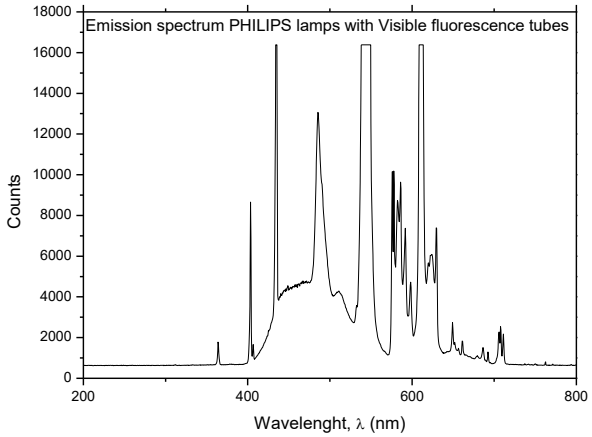

Figure 6.1 Emission spectrum of Philips lamps (Solarium HB 175) equipped with four fluorescence visible tubes.

As can be observed for the Philips lamp the main emission range is between 400 and 640 nm with four maxima at: 435 nm, 490 nm, 545 nm, the most intense, and 612 nm. That is, this lamp provides a very dispersed irradiation.

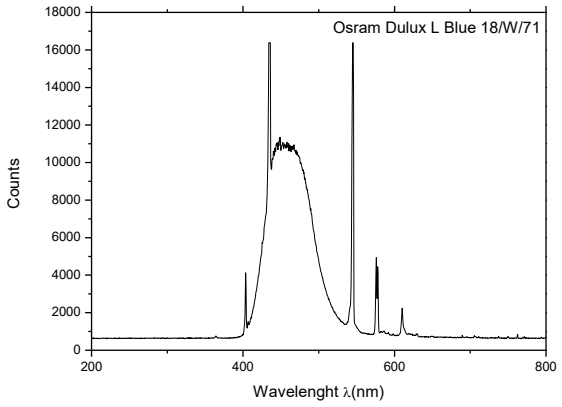

Figure 6.2 Osram Dulux L Blue emission spectrum

The Osram lamp has a more concentrated emission in the range from 400 to 550 nm with two maxima: one at 435 and the other one at 546 nm.

Table 6.1 Main emission data of the lamps used.

	Power W/m^2	Photon/cm^2/s
Philips Vis T5 Solarium HB175	24.9	$6.13x10^{15}$
Osram Dulux L Blue	31.8	$7.32x10^{15}$

6.2.2 Slurry tests

The catalyst load was only 0.3 g/L and the concentration of 4-Nitrophenol tested varied from 10 to 50 mg/L (from $7x10^{-5}$ to $4x10^{-4}$ mol/L). All the solutions were sonicated for 2 minutes before irradiation and stirred at 700 rpm with a magnetic stirrer during the reaction time.

The samples were stirred in the dark (lamps off, reactor covered with an aluminum sheet) for 30 minutes, to allow adsorption of the pollutant onto the catalyst's surface.

Once finished the adsorption process, an oxidising agent (H_2O_2) was added to the suspension in a concentration of 0.006 M. Then the pH was measured and adjusted to pH around 5 in some reactions, others were allowed to develop natural pH values. These values were recorded, in any case, during the reaction to reach a better comprehension of the process.

The configuration of the photoreactor included reflecting planes placed inside the reaction chamber. These collectors guaranteed a greater exploitation of the photons emitted and so ensured an increase in the quantum efficiency of radiation.

The total irradiation time was 240 minutes (4h); samples were extracted at regular time intervals with a syringe and filtrated with a Millipore needle filter with a pore diameter of 0.45 μm in order to eliminate the catalyst from the suspensions. The samples were afterwards analysed by HPLC and/or by TOC. These measurements were conducted immediately when possible or kept in the fridge until analysis, in order to preserve them, preventing the progress of the reaction or unwanted degradation processes.

6.2.3 Fixed-bed tests

Lanthanum ferrite was tested in the form of nanostructured $LaFeO_3$ powder on dip-coated ceramic foams with a macroporous density of 10 ppi. Dip-coating technique allows impregnating of the support surface with the catalyst by dipping it into a $LaFeO_3$ suspension and undergoing a thermal treatment for solvent evaporation and a final washing by sonication. More information about the operating method can be found in section 3.5.

The preliminary studies for the choice of the better dip-coating conditions for the catalyst deposition consisted of changing the number of the programed cycles (immersion/emersion/standing) in the dip-coater and grinding or not the lanthanum ferrite.

The number of the cycles carried out were 3, 5 and 7. The first conclusion was that not grinding the catalyst led to more loss of catalyst during the washing with water milli-Q grade by sonication and the final quantity of supported $LaFeO_3$ was minor. The second conclusion was that there is a limit in the quantity that can be supported: the final amount supported increased from the first 3 to 5 cycles but after the 5^{th} cycle this amount was nearly constant.

So that, it was decided to apply five cycles and to use the ground material. The rate of catalyst over the foam was approximately a 1% of the total weight.

Photocatalytic ceramic blocks were introduced in a beaker and placed in a photoreactor, subjected to visible radiation and magnetic stirring during the reaction time.

4-Nitrophenol was used as model contaminant for comparing different aspects of the photoreaction.

The amount of catalyst supported onto the foam ranged from 110 mg to 160 mg but the degradation rate seems to be independent on the catalyst load, within a certain range. This fact can be explained in terms of availability of active sites on $LaFeO_3$ surface and the penetration of activating light into the foam structure [59]. The light arrives at the surface of the ceramic foam and only in part it penetrates inside the pores. Moreover, probably there is some catalyst covered by more external layers that does not receive the light and that is not in contact with the pollutant so does not react. The external walls of the foam are the most exposed to the radiation and to the solution, the ratio between external and total surface is very low. To

optimize the photocatalyzer performance the most part of it should be both reached by light and in contact with the pollutant; this is true for the photocatalyzer deposited onto the external surface of the foam, much less so inside the pores. Some light transmission takes place due to the white color of the ceramic foam, but for improving the contact with the pollutant an appropriate experimental setup must be devised.

Two different reactors were employed:

_Immobilized ceramic foam photoreactor: where the photocatalytic blocks remain fixed and the solution is stirred.

_Rotating ceramic foam photoreactor: the blocks rotate around a vertical axle, the solution is kept in agitation by the foam movement.

6.2.3.1 Immobilized ceramic foam photoreactor

The foam was introduced in a beaker and kept separated from the bottom by inox steel wires so that a magnet could be introduced under the photocatalytic block to stir the solution.

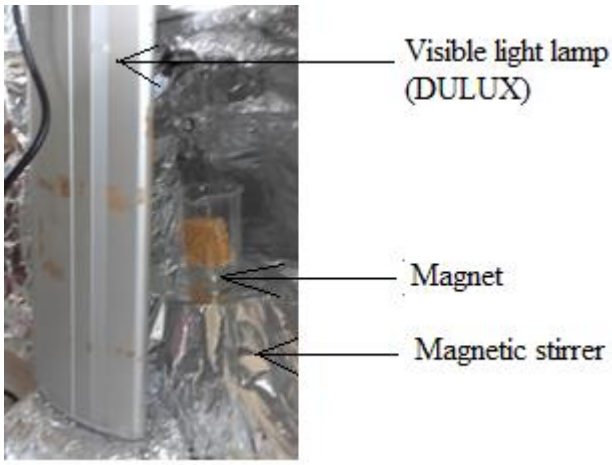

Figure 6.3 Immobilized ceramic foam photoreactor.

A volume of 220 mL of 4-Nitrophenol in water (10 mg/L or 50 mg/L) was introduced in a beaker where was placed the foam. Then the stirring started and for 30 minutes the system was maintained in the dark. After this period, necessary to achieve an equilibrium between adsorption and desorption of the pollutant on the catalyst surface, hydrogen peroxide (H_2O_2) was added to reach a concentration of 0.006 M. The lamps were turned on and the photoreaction started. At fixed intervals of time the solution was sampled and analysed by HPLC. The degradation rate was very poor in this phase in contrast with the slurry tests results so a new reactor was projected: a rotating foam photoreactor.

6.2.3.2 Rotating ceramic foam photoreactor

An innovative reactor was designed to achieve optimum mixing and diffusion of the solution among the channels of the foam and to

improve the surface exposure to light. The reactor system used in the previously described tests seemed non-adequate to the geometry of the foam. It can be affirmed that almost only the six external faces of the parallelepipedal support worked as photocatalyst. The water flow in the internal channels could be near zero.

In the new reactor, the foam was hung from a rotating shaft by a nylon thread, so that the rotation was integral with the axis. The rotation velocity was measured and kept constant.

The typical reaction was the same of the one used in the immobilized foam photoreactor and detailed above.

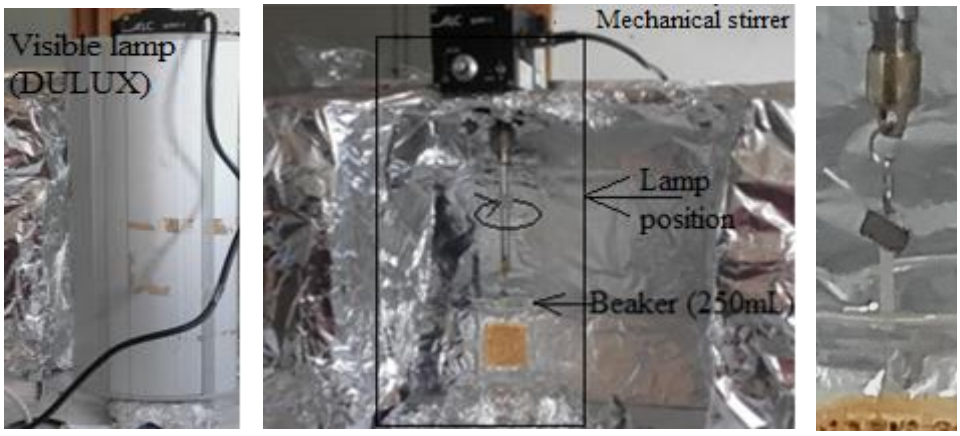

Figure 6.4 Rotating ceramic foam photoreactor. On the left, the lamp that was put in front of the foam; on the middle, the interior of the reactor with a rectangle indicating the position of the lamp; on the right, a zoom of the union between the foam and the axle.

6.3 Results and Discussion

6.3.1 Pollutant photocatalytic degradation

SLURRY TESTS

The objectives of these tests were three: to find the better conditions for the degradation activity of the photocatalyst, to be able to compare the performances of the catalyst in slurry and the deposited one and to compare the degradation capability of the three characterized batches.

Irradiation influence:

The two lamps whose spectrum was analysed, Figure 6.1 and 6.2, were tested in the degradation of 50 g/mL of 4-Nitrophenol solution at pH 5.3 and the results were similar. The Osram Dulux lamp, that led to slightly better results, was chosen mainly because it heated the reactor less.

pH influence:

A battery of tests was carried out with natural pH, around 6.2. The results were very poor with a degradation rate of 20% aprox. of the pollutant presents in the solution.

When the pH was decreased to 4.8 the reaction rate increased up to achieve a total elimination of the pollutant after 3 hours (C_0=50 mg/L of 4-Nitrophenol)

The pH diminution was carried out by the addition of H_2SO_4 and it was difficult to reach stable pH level probably because of the carbonate groups present in the catalyst. The pH still increasing after each volume of acid solution added until the complete neutralization of these carbonates. Different batches required different acid solution volumes to reach the same pH values, this is a confirmation of the differences in their compositions found through the thermogravimetric analysis.

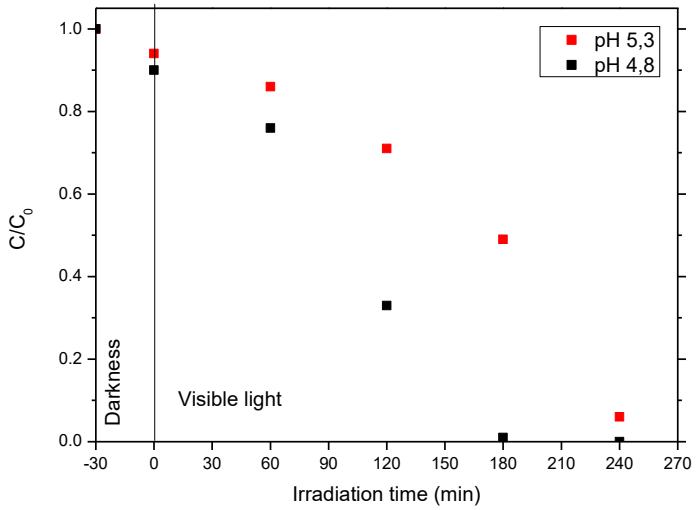

Figure 6.5: Comparison between the photodegradation of 4-Nitrophenol (50 ppm) reached with two initial pH: pH_0 4.8 in black and pH_0 5.3 in red.

Initial concentration of the pollutant influence:

The degradation rate increased with the increase of the initial concentration of 4-nitrophenol. This fact have been found before [45] where the degradation rate of 4-chlorophenol, using $LaFeO_3$ as catalyst, increased when the initial concentration was doubled. That paper reports how further increment of concentration drove to a diminution of degradation rate.

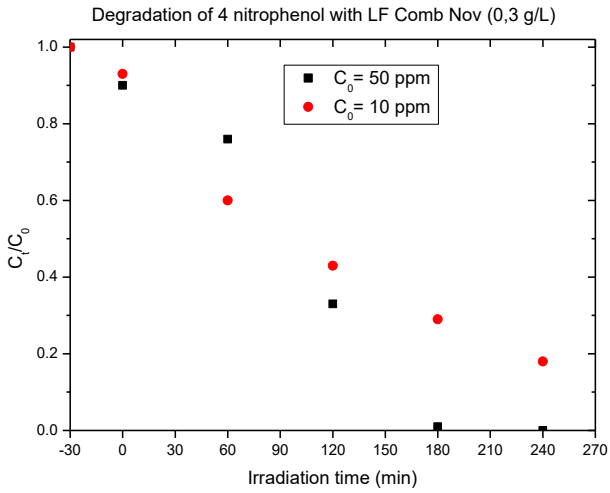

Figure 6.6 Degradation of 4-Nitrophenol with the same photocatalyst and different initial concentration: C_0 =10 and C_0 =50 mg/L, pH_0 4.8.

As can be observed in the graphs the curves trends are different; it could be interesting to verify what happens when the high concentration solution changes from 10 to 0 mg/L. Maybe the shape of the curve in this interval is similar to that observed starting with a pollutant concentration of 10 mg/L.

Batches of catalyst influence:

This part of the work was conducted to determinate if the quality of the photocatalyst produced in large quantities remained unchanged. The effectiveness of C8 and C10 batches was the same for all the tests, changing pH and initial pollutant concentration. Best performances were shown by the C12 + C13 batches. This fact maybe due to the quantity added of H_2SO_4 solution that was higher for this batch to reach the same pH value. Therefore, more SO_4^{2-} ions were introduced in the solution, they can improve the photoreaction rate. But another possibility can be the oxygen vacancy suspected in this batch from the scanning electron micrography (SEM-BSE).

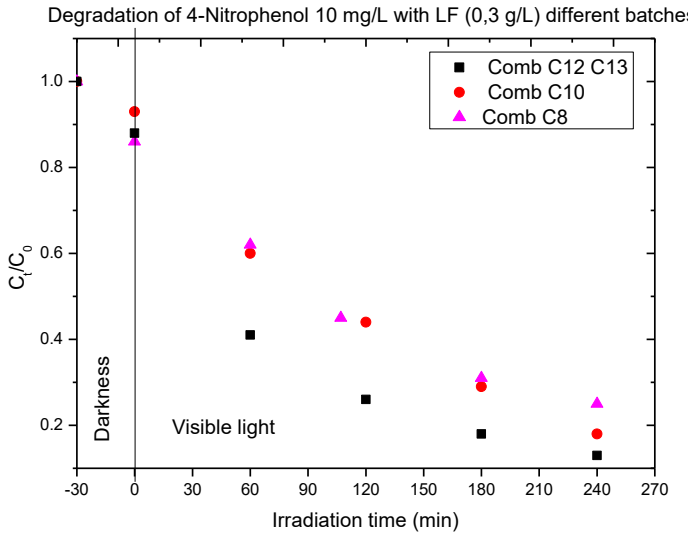

Figure 6.7 Degradation of 4-Nitrophenol (10 mg/L, pH=4.8) with three different batches of photocatalyst, synthesized by the same procedure.

SUPPORTED PHOTOCATALYST TEST

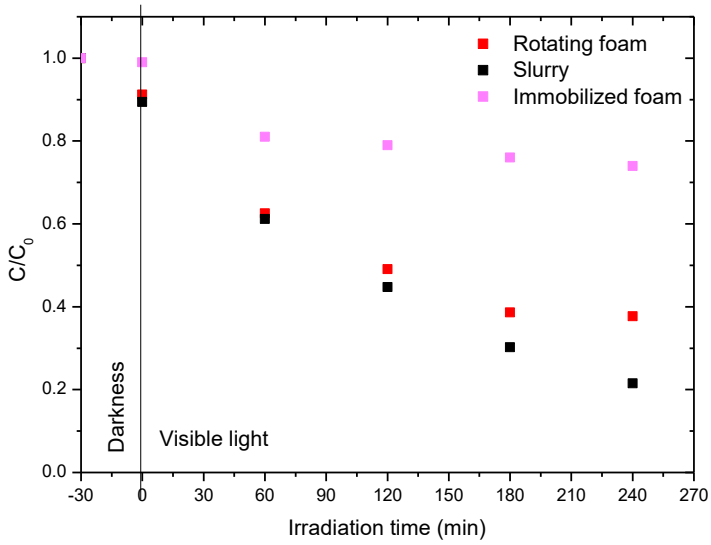

Figure 6.8 Degradation of 4-Nitrophenol (10 mg/L); catalyst in slurry (black), foam in rotating reactor (red) and foam in immobilized reactor (pink).

Here the results of the degradation of 4-Nitrophenol with the catalytic foam are shown. The load of catalyst was around 0.7 g/L. As explained before, two methods were used: the first with immobilized foam, the standard operational method used in our laboratory, and the second where the foam was kept in a constant rotational movement. The contact between the catalyst and the pollutant increases and the light radiation arrives more homogeneously at the surface of the catalyst with the second system.

Reuse cycles

During the firsts tests the foam was drawn from the reaction beaker and reused without further treatment. The degradation rate decreased from the third cycle. One explanation for the loss of activity is that the catalyst might have been poisoned by the pollutant or the byproducts of the reaction, so it might be necessary to clean the foam after each use. Trying to recover the photoactivity, the material was washed in two ways: with water and with H_2O_2-visible light irradiation.

Washing with H_2O

The ceramic block was introduced in the photoreactor with 220 mL of water and kept in the rotation mode and in the dark for one hour. The water was changed every fifteen minutes.

Washing with H_2O_2 - visible light.

The ceramic block was introduced in 220 mL of a 0,006 M solution of H_2O_2 in water and kept in the rotation mode for one hour with visible irradiation.

The results were not very encouraging with what is thought to be more effective cleaning with water after each use and not only when the foam is inactive. Anyway, the first method of regeneration, washing with water, was somewhat better.

Washing with H_2O – after each cycle

When the foam was washed with water milli-Q after cycle, with the spin movement for 30 minutes, the loss of activity initiated from the fourth cycle. From the first to the third cycle, effectiveness increased. The added volume of acid solution to reach pH 4.8 was lower from the second cycle, so the carbonate present in the foam that hinders the pH stability had been neutralized.

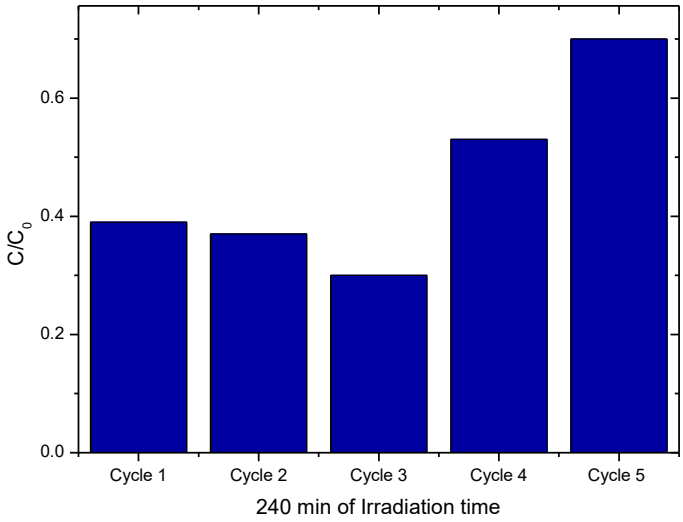

Figure 6.9 Degradation of 4-Nitrophenol (10 mg/L) with the spin-foam, five cycles. pH 4.8

6.3.2 Foam microanalysis

In order to determine the reason why the process efficacy decreases after the third cycle, SEM analysis were conducted for not used samples and for employed ones. From the Figure 6.10 no conclusions can be drawn regarding the distribution or the remaining quantity of catalyst because this micro distribution changes from one zone to another and, due to the operating method, it is not possible to examine the same area before and after use. However, some information can be obtained from the backscattered electron images (BSE): the ratio between Fe:La varied from 0.9 before the use of the foam to 0.5 in some areas or 1.3 in others in the foam after the use. This fact indicates that there might have been a catalyst degradation during the reactions and provides an explanation for the reduced activity of the photocatalyst supported. This information will be compared with SEM analyses all around the surface foam to clarify the process.

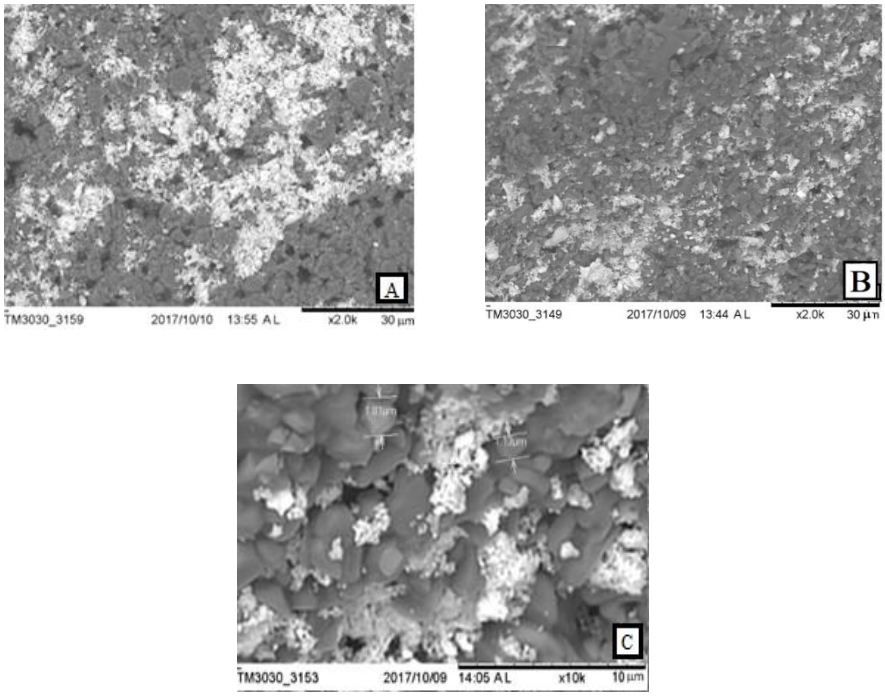

Figure 6.10 Foam SEM micrographs. A) Sample not employed (x2K), B) Sample after five cycles (x2K) and C) Sample after five cycles (x10K) with some measurements.

6.3.3 Atomic Absorption Test

Atomic Absorption test carried out to determine the presence of leached iron in the solution after the degradation tests gave as result: 0.024 mg/L. Considering the solution conditions, only 0.0145 wt% of the iron present has been dissolved. This quantity is too small to contribute to the degradation rate as a homogeneous Fenton reaction. Other authors report that $LaFeO_3$ present no loss of iron ions during the reactions and prove it with the Atomic Absorption Spectrometer.

6.4 Conclusions

Lowering the pH of the solutions led to better results, passing from a 20-30% of degradation after 4 hours of irradiation at natural pH values to a 100 % of degradation after only 3 hours at pH of 4,8 (C_0= 50 ppm). From the TOC analysis, it was found that never was reached a complete mineralization; for example, when the concentration of 4-Nitrophenol was zero the final TOC was around 50% of the initial one.

In the slurry tests the degradation was higher for higher initial concentration of the pollutant (50 mg/L). while with the foam the degradation was similar for 50 and 10 mg/L of initial concentration.

The different batches showed slight differences during the degradation tests. The best results were for the C12+C13 batch but the reason it not clear yet. Two are the possibilities proposed: the oxygen vacancy suspected from the BSE analysis or the higher amount of SO_4^{2-} added when the pH was reduced by a H_2SO_4 solution, more acid solution was required to reach the same pH value. These ions can enhance the oxidation process.

The supported catalyst (0.7 g/L) degraded the 4-Nitrophenol 10 mg/L solution as well as the catalyst in slurry (0.3 g/L).

Three reuse cycles were achieved with good performances. From the fourth the results decrease. The reason and a possible reactivation technique of this early inactivation has not been yet found. A probable degradation of the catalyst in the acid media is being considered.

The reaction mechanism involves a photo Fenton-like heterogeneous process but not homogeneous contribution is present, this fact is demonstrated with the low presence of iron dissolved into the solution.

CHAPTER 7 CONCLUSIONS AND FUTURE PERSPECTIVES

Characterization of three different batches of $LaFeO_3$ by XRD, SEM, FTIR, DRS, and TGA was carried out to better understand the photocatalytic process and the synthesis control when the quantities of the batches were increased. The reproducibility of the synthesis process of the catalyst used here has been largely studied for low and constant quantities batches. On the basis of the variations found between them, investigations can be addressed to explain them in order to modify the synthesis phase.

A more detailed thermogravimetric study seems very interesting to determine the optimum calcination temperature of the lanthanum ferrite photocatalyst. So, a TGA analysis will be executed with a non-calcined $LaFeO_3$ powder; by this technique, combined with FTIR studies, it will be possible to find the temperature at which byproducts of the synthesis reaction such as nitrates and carbonates are eliminated. These impurities on the surface lead to pH modifications and obstruct the pollutants adsorption by the photocatalyst, therefore their reduction will be an important aim in the future.

The photocatalytic paint (LF) was very interesting not only for its successful self-cleaning performances but also for the weather resistance it demonstrated. The addition of 1 wt% of $LaFeO_3$ powder

confers photocatalytic properties to the reference paint without loss of its initial performances. Now interest will be pointed in the increase of the percentage of the catalyst to enhance its photocatalytic properties. A handicap of this visible sensitive photocatalyst is the brown color of lanthanum ferrite, so that the more its quantity in the paint recipe, the browner will be the tone of the final paint.

The preliminary test with the supported ceramic foam with the elimination of 4-Nitrophenol resulted very positive and encouraging; the degradation rate was very similar to the slurry tests. The degradation of other pollutants will be carried up to develop the photocatalytic foams. Ibuprofen and some pesticides will be degraded.

Degradation studies with natural sun irradiation will be carried out also.

An important objective to achieve an industrial application of the photocatalyst foam studied is the increase of reuse cycles. Presently we reached only three cycles of reuse. In this address, a better understanding of the reasons of the performance loss is desired.

The SEM observations of the supported ceramic foam showed a very thin and non-homogeneous film of lanthanum ferrite. As explained previously, a number of cycles in the dip-coater exceeding five don’t lead to an increase in the deposited amount; another way to achieve a higher deposition could be to repeat the five cycles of the dip-coating process once the foam has been washed, dried and weighed. In this way, it could be possible to load the foam with a

well-defined amount of lanthanum ferrite by continuing the deposition up to the desired weight.

Testing other supports is also in program. In particular, instead of using a commercial ceramic foam as support, it would also be possible to prepare different foams by varying the ceramic material, the dimensions and shape of the foam samples, in order to tailor the process to the application requirements.

PAPER

CHEMICAL ENGINEERING TRANSACTIONS
VOL. 57, 2017
A publication of AIDIC
The Italian Association of Chemical Engineering
Online at www.aidic.it/cet
Guest Editors: Sauro Pierucci, Jiří Jaromír Klemeš, Laura Piazza, Serafim Bakalis

ISBN 978-88-95608- 48-8; **ISSN** 2283-9216

Simulated Weathering Tests of Photocatalytic Paint Containing $LaFeO_3$

Elena de la Fuente García[a], Veronica Carrara[a], Francesca Fontana[a], Isabella Natali Sora*[a]

[a]Università di Bergamo, Dipartimento di Ingegneria e Scienze Applicate, Viale Marconi 5, 24044 Dalmine BG, Italy
isabella.natali-sora@unibg.it

The effects of simulated weathering tests on water paints based upon a silicate binder, containing a $LaFeO_3$ photocatalyst, were investigated by measuring their self-cleaning performances. Paint samples were exposed to accelerated ageing tests using a climatic chamber, which simulated weathering effects such as UV radiation, rainwater and conspicuous temperature and humidity variations. Samples were subsequently stained by Procion Red PX4B dye and the color degradation of the taint onto the solid phase was followed through UV–vis diffuse reflectance spectra (DRS). The dye discoloration percentage after 360 h visible light irradiation was 78 % for not weathered samples, and 67 % for weathered ones.

BIBLIOGRAPHY

[1] T. Caronna, F. Fontana, I. N. Sora, and R. Pelosato, “Chemical synthesis and structural characterization of the substitution compound $LaFe_{1-x}Cu_xO_3$ (x = 0 – 0 . 40),” vol. 116, pp. 645–648, 2009.

[2] I. Natali Sora, V. Felice, F. Zurlo, S. Licoccia, and E. Di Bartolomeo, “Characterization of tantalum doped lanthanum strontium ferrite as cathode materials for solid oxide fuel cells,” *J. Alloys Compd.*, vol. 648, pp. 154–159, 2015.

[3] I. N. Sora *et al.*, “Photoelectrochemical properties of doped lanthanum orthoferrites,” *Electrochim. Acta*, 2013.

[4] I. Natali Sora and D. Fumagalli, “Fast photocatalytic degradation of pharmaceutical micropollutants and ecotoxicological effects,” *Environ. Sci. Pollut. Res.*, 2017.

[5] W. Zhang, B. Jia, and Q. Wang, “Visible-light sensitization of TiO_2 photocatalysts via wet chemical N-doping for the degradation of dissolved organic compounds in wastewater treatment : a review,” *J. Nanoparticle Res.*, vol. 17, no. 5, pp. 1–12, 2015.

[6] D. Y. G. and K. S. S. P. Wyness, J. F. Klausner, “Performance of Nonconcentrating Solar Photocatalytic Oxidation Reactors: Part II—Shallow Pond Configuration,” *J. Sol. Energy Eng*, vol. 116, no. 1, pp. 8–13, 1994.

[7] D. Y. G. and K. S. S. P. Wyness, J. F. Klausner, “Performance of Nonconcentrating Solar Photocatalytic Oxidation Reactors: Part I—Flat-Plate Configuration,” *J. Sol. Energy Eng*, vol. 116, pp. 2–7, 1994.

[8] F. S. Braz, M. R. A. Silva, F. S. Silva, S. J. Andrade, A. L. Fonseca, and M. M. Kondo, “Photocatalytic Degradation of Ibuprofen Using TiO_2 and Ecotoxicological Assessment of

Degradation Intermediates against Daphnia similis," no. May, pp. 620–626, 2014.

[9] D.B.Weichgrebe,"Chemish-Oxidativen Abwasserbehandlung. Dissertation," *Clausthal*, 1984.

[10] C.C.Way., T.Y., Wan, "Heterogeneous photocatalytic oxidation of phenol with titanium dioxide powders," *Ind. Eng. Chem. Res.*, pp. 1293–1300, 1991.

[11] R. Munter, "Advanced oxidation processes – current," pp. 59–80, 2001.

[12] K. Gao and S. Li, "Applied Surface Science Multi-modal TiO_2 – $LaFeO_3$ composite films with high photocatalytic activity and hydrophilicity," *Appl. Surf. Sci.*, vol. 258, no. 17, pp. 6460–6464, 2012.

[13] J. X. XinLi, Rongchen Shen, Song Ma, Xiaobo Chen, "Graphene-based heterojunction photocatalysts," *Appl. Surf. Sci.*, 2017.

[14] D. F. A K Kulkarni, F T Ciacchi, S Giddey, C Munnings, S P S Badwal, J Kimpton, "MIXED CONDUCTING ANODE FOR DIRECT CARBON FUEL CELL," *Int. J. Hydrogen Energy*, vol. 37, no. 24, pp. 19092–19102, 2012.

[15] G. Physics, E. Alekseevna, and T. Russian, "Phase diagram of the $LaFeO_3$-$LaSrFeO_4$ system," no. December, pp. 1–4, 2006.

[16] S. L. Francesca Zurlo, Elisabetta Di Bartolomeo, Alessandra D'Epifanioa Valeria Felice Isabella Natali Sora, LucaTortora, "$La_{0.8}Sr_{0.2}Fe_{0.8}Cu_{0.2}O_{3-\delta}$ as 'cobalt-free' cathode for $La_{0.8}Sr_{0.2}Ga_{0.8}Mg_{0.2}O_{3-\delta}$ electrolyte," *J. Power Sources*, vol. 271, pp. 187–194, 2014.

[17] Y. Du Jing Zhao, Yinping Liu, Xiaowei Li, Geyu Lu, Lu You, Xishuang Liang, Fengmin Liu, Tong Zhang, "Highly sensitive humidity sensor based on high surface area mesoporous $LaFeO_3$ prepared by a nanocasting route," *Sensors Actuators B Chem.*, vol. 181, 2013.

[18] K. Rusevova, R. Köferstein, M. Rosell, H. H. Richnow, F. Kopinke, and A. Georgi, "$LaFeO_3$ and $BiFeO_3$ perovskites as

nanocatalysts for contaminant degradation in heterogeneous Fenton-like reactions," vol. 239, pp. 322–331, 2014.

[19] D. Sannino, V. Vaiano, L. A. Isupova, and P. Ciambelli, "Photo-Fenton Oxidation of Acetic Acid on Supported $LaFeO_3$ and Pt/$LaFeO_3$ Perovskites," *J. Adv. Oxid. Technol.*, vol. 15, no. 2, pp. 294–300, 2012.

[20] V. V. Sannino Diana, Isupova, and C. Paolo, "Heterogeneous Photo-Fenton Oxidation of Organic Pollutants on Structured Catalysts," *J. Adv. Oxid. Technol.*, vol. 15, no. 2, pp. 294–300, 2012.

[21] H. F. Shudan Li, Liqiang Jing, Wei Fu, Libin Yang, Baifu Xin, "Photoinduced charge property of nanosized perovskite-type $LaFeO_3$ and its relationships with photocatalytic activity under visible irradiation," *Mater. Res. Bull.*, vol. 42, no. 2, pp. 203–212, 2007.

[22] H. Su, L. Jing, K. Shi, C. Yao, and H. Fu, "Synthesis of large surface area $LaFeO_3$ nanoparticles by SBA-16 template method as high active visible photocatalysts," *J. Nanoparticle Res.*, 2010.

[23] C. V. and N. P. S. Thirumalairajan, K. Girija, Neha Y. Hebalkar, D. Mangalaraj, "Shape evolution of perovskite $LaFeO_3$ nanostructures: a systematic investigation of growth mechanism, properties and morphology dependent photocatalytic activities," *RSC Adv.*, vol. 3, no. 20, pp. 7549–7561, 2013.

[24] N. B. Kulamani Parida, K. H. ReddySatyabadi Martha, "Fabrication of nanocrystalline $LaFeO_3$: An efficient sol–gel auto-combustion assisted visible light responsive photocatalyst for water decomposition," *Int. J. Hydrogen Energy*, vol. 35, no. 22, pp. 12161–12168, Nov. 2010.

[25] L. N. Tijare S, Joshi M, Padole P, Mangrulkar P, Rayalu S, "Photocatalytic hydrogen generation through water splitting on nano-crystalline $LaFeO_3$ perovskite," *Int. J. Hydrogen Energy*, vol. 37, no. 13, pp. 10451–10456, Jul. 2012.

[26] K. Peng, L. Fu, H. Yang, and J. Ouyang, “Perovskite LaFeO 3 /montmorillonite nanocomposites: synthesis, interface characteristics and enhanced photocatalytic activity,” 2016.

[27] K. Wang *et al.*, “Immobilizing $LaFeO_3$ nanoparticles on carbon spheres for enhanced heterogeneous photo-Fenton like performance,” *Appl. Surf. Sci.*, vol. 404, pp. 138–145, 2017.

[28] “ISO 22197-1: 2016 ‘(Fine ceramics, advanced technical ceramics) – Test method for air-purification performance of semiconducting photocatalytic materials – part 1: Removal of nitric oxide’, ISO, Geneva, 2016.” .

[29] “ISO 22197-2: 2011, ‘Fine ceramics, advanced technical ceramics) – Test method for air-purification performance of semiconducting photocatalytic materials – part 2: Removal of acetaldehyde. ISO, Geneva, 2011.” .

[30] “ISO 22197-3: 2011, ‘Fine ceramics, advanced technical ceramics) – Test method for air-purification performance of semiconducting photocatalytic materials – part 3: Removal of toluene’. ISO, Geneva, 2011.”

[31] “ISO 27448:2009 Fine ceramics (advanced ceramics, advanced technical ceramics) -- Test method for self-cleaning performance of semiconducting photocatalytic materials -- Measurement of water contact angle.” .

[32] “ISO 10678:2010 Fine ceramics (advanced ceramics, advanced technical ceramics) -- Determination of photocatalytic activity of surfaces in an aqueous medium by degradation of methylene blue.” .

[33] “ISO 27447:2009 Preview Fine ceramics (advanced ceramics, advanced technical ceramics) -- Test method for antibacterial activity of semiconducting photocatalytic materials.”

[34] “ISO 10677:2011 Preview Fine ceramics (advanced ceramics, advanced technical ceramics) -- Ultraviolet light source for testing semiconducting photocatalytic materials.” .

[35] F. B. L. Bergamonti, G. Predieri, Y. Paz, L. Fornasini, P.P. Lottici, “Enhanced self-cleaning properties of N-doped TiO_2

coating for Cultural Heritage," *Microchem. J.*, vol. 133, pp. 1–12.

[36] Otmar Geiss Carmen Cacho Josefa Barrero-Moreno Dimitrios Kotzias, "A mechanism based on Photocatalytic degradation of organic paint constituents-formation of carbonyls," *Build. Environ.*, vol. 48, pp. 107–112, 2012.

[37] Joonas Auvinen Leif Wirtanen, "The influence of photocatalytic interior paints on indoor air quality," *Atmos. Environ.*, vol. 42, pp. 4101–4112, 2008.

[38] L. Caballero, K. A. Whitehead, N. S. Allen, and J. Verran, "Photoinactivation of Escherichia coli on acrylic paint formulations using fluorescent light," *Dye. Pigment.*, vol. 86, no. 1, pp. 56–62, 2010.

[39] A. Markowska-szczupak, K. Ulfig, B. Grzmil, and A. W. Morawski, "A preliminary study on antifungal effect of TiO_2 -based paints in natural indoor light," pp. 53–57, 2010.

[40] M. Baudys, J. Krýsa, M. Zlámal, and A. Mills, "Weathering tests of photocatalytic facade paints containing ZnO and TiO_2," *Chem. Eng. J.*, vol. 261, pp. 83–87, 2015.

[41] M. Baudys, J. Kr??sa, and A. Mills, "Smart inks as photocatalytic activity indicators of self-cleaning paints," *Catal. Today*, 2016.

[42] G. R. C. Colleoni, M.R. Massafra, "Photocatalytic properties and optical characterization of cotton fabric coated via sol–gel with non-crystalline TiO_2 modified with poly(ethylene glycol)," *Surf. Coatings Technol.*, vol. 207, pp. 79–88, Aug. 2012.

[43] Aref Shokri, "Degradation of 4-Nitrophenol from industerial wastewater by nano catalytic Ozonation Young Researchers and Elite Club, Arak Branch, Islamic Azad University, Arak, Iran Re," *Int. J. Nano Dimens.*, vol. 7, no. 2, pp. 160–167, 2016.

[44] D. K.Ray, "Photodegradation kinetics of 4-nitrophenol in TiO_2 suspension," *Water Res.*, vol. 32, no. 22, pp. 3223–3234.

[45] S. G. Babu, P. Aparna, G. Satishkumar, M. Ashokkumar, and B. Neppolian, “Ultrasound-assisted mineralization of organic contaminants using a recyclable $LaFeO_3$ and Fe^{3+}/persulfate Fenton-like system,” *Ultrason. Sonochem.*, 2017.

[46] F. M. P. Kubelka, “Ein Beitrag Zur Optik Der Farbanstriche,” *Z. Techn. Phys*, vol. 12, pp. 593–601, 1931.

[47] R. Belloli, B. Barletta, E. Bolzacchini, S. Meinardi, M. Orlandi, and B. Rindone, “Determination of toxic nitrophenols in the atmosphere by high-performance liquid chromatography,” *J. Chromatogr. A*, vol. 846, no. 1–2, pp. 277–281, 1999.

[48] C. M. Malengreaux, A. Timmermans, and S. L. Pirard, “Optimized deposition of TiO_2 thin films produced by a non-aqueous sol-gel method and quantification of their photocatalytic activity Key words.”

[49] R.Molina, Y.Segura, F.Martínez, J.A.Melero, “Immobilization of active and stable goethite coated-films by a dip-coating process and its application for photo-Fenton systems,” *Chem. Eng. J.*, vol. 203, pp. 212–222, 2012.

[50] J.-M. Tulliani, M. M. Natile, L. Tortora, and I. Natali Sora, “Ageing of lanthanum strontium copper orthoferrite powders for sensing layers,” *Chem. Eng. Trans.*, vol. 43, no. 2013, pp. 1807–1812, 2015.

[51] H. Tan *et al.*, “Oxygen Vacancy Enhanced Photocatalytic Activity of Pervoskite $SrTiO_3$,” pp. 19184–19190, 2014.

[52] W. El-Alami *et al.*, “TiO_2 and F-TiO_2 photocatalytic deactivation in gas phase,” *Chem. Phys. Lett.*, vol. 684, pp. 164–170, 2017.

[53] A. C. Sola *et al.*, “Differences in the vapour phase photocatalytic degradation of ammonia and ethanol in the presence of water as a function of TiO_2 characteristics and the presence of O_2,” *Catal. Today*, vol. 266, pp. 53–61, 2016.

[54] S. P. authorSupree P. M. Rujirawat, “Structure, optical and magnetic properties of $LaFeO_3$ nanoparticles prepared by

polymerized complex method," *J. sol gel Sci. -technology*, vol. 71, no. 2, pp. 334–341.

[55] H.-S. Kim *et al.*, "Lead iodide perovskite sensitized all-solid-state submicron thin film mesoscopic solar cell with efficiency exceeding 9%.," *Sci. Rep.*, vol. 2, no. 7436, p. 591, 2012.

[56] B. Daniotti, S. L. Spagnolo, and R. Paolini, "Climatic Data Analysis to Define Accelerated Ageing for Reference Service Life Evaluation," no. May, 2008.

[57] L. A. F. Parrino, E. García-López, G Marci, L Palmisano, V. Felice, I. Natali-Sora, "Cu-substituted lanthanum ferrite perovskites: Preparation, characterization and photocatalytic activity in gas-solid regime under simulated solar light irradiation," *J. Alloys Compd.*, vol. 682, pp. 686–694, Oct. 2016.

[58] G. Germinario, I. D. van der Werf, and L. Sabbatini, "Chemical characterisation of spray paints by a multi-analytical (Py/GC–MS, FTIR, μ-Raman) approach," *Microchem. J.*, vol. 124, pp. 929–939, Jan. 2016.

[59] M. M. Micó *et al.*, "Heterogeneous Photocatalysis Using Supported Nano-TiO_2 for Micropollutant Elimination."

ACKNOWLEDGEMENTS

Risulta molto difficile ringraziare con poche parole le persone che mi hanno aiutata, sostenuta e sopportata durante questo percorso qualche volta difficile e impegnativo ma sempre molto gratificante e costruttivo. Le persone che ho avuto la fortuna di incontrare durante questi tre anni rimarranno per sempre nel mio cuore.

Prima di tutto, vorrei ringraziare le due professoresse che mi hanno dato l'opportunità di svolgere questo lavoro e aiutato tantissimo a portarlo avanti: la Prof.ssa Francesca Fontana e la Prof.ssa Isabella Natali-Sora.

Questo percorso non avrebbe mai avuto inizio senza la persona che mi ha accolta in questo Dipartimento circa dodici anni fa per realizzare la mia tesi di laurea, offrendomi in seguito l'opportunità di continuare l'attività di ricerca preso il suo laboratorio durante diversi anni: il Prof. Tullio Caronna.

Un speciale e affettuoso grazie ai miei compagni di laboratorio a Dalmine che tanto mi hanno sostenuta, aiutata, rallegrato ogni giorno, ascoltata e consigliato duranti i miei momenti più difficili: Veronica Carrara e Damiano Cancogni. Ai miei cari tesisti: Marius Eteme Minkada e Youssef Ait.

Ringrazio a tutto il personale che mi ha accolto preso l'Università di Padova e il Politecnico di Milano.

L'ultimo periodo della mia tesi l'ho trascorso alla "Universidad de Las Palmas de Gran Canaria" grazie alla disponibilità dei professori

responsabili del gruppo CIDIA. A loro devo gran parte di questa tesi e della voglia crescente di fare ricerca: Prof. Oscar González, Prof. Javier Araña y Prof.ssa Elisenda Pulido.

Là ho avuto la fortuna di trovare Ari, Maria José, Nereida, Davinia y Omayra grandi maestre, magnifiche e instancabili collaboratrici e, spero, amiche per sempre.

Finalmente vorrei ringraziare tutta la mia famiglia che con la loro forza e pazienza mi ha sostenuta, facendo possibile arrivare a concludere questo lavoro. Specialmente ai miei figli Daniele e Pablo che insieme a mio marito Enrico hanno perso un po' della dedicazione che meritavano e che tanto desidero darli.

Per finire, ringrazio l'Università di Bergamo per la borsa di studio che mi è stata concessa.